INL/EXT-05-00886

Engineering and Physics Optimization of Breed and Burn Fast Reactor Systems – Annual and Final Report

NERI Project No. 2002-05

Theron Marshall
James Parry
Kevan D. Weaver

October 2005

The INL is a U.S. Department of Energy National Laboratory
operated by Battelle Energy Alliance

INL/EXT-05-00886

Engineering and Physics Optimization of Breed and Burn Fast Reactor Systems – Annual and Final Report

NERI Project No. 2002-05

Theron Marshall
James Parry
Kevan D. Weaver

October 2005

Idaho National Laboratory
Idaho Falls, Idaho 83415

Prepared for the
U.S. Department of Energy
Under DOE Idaho Operations Office
Contract DE-AC07-05ID14517

Table of Contents

1. Executive Summary 1
2. Task A: Core Physics 2
2.1 Model Details 2
2.2 Neutronics Results 4
2.3 Plutonium Fueled Depletion Model 7
2.4 14% Enriched Uranium Fueled Depletion Model 12
2.5 7% Enriched Uranium Fueled Depletion Model 16
2.6 Conclusions 20
3. Tasks B and C: Core Thermal Hydraulics and Plant Design 21
3.1 Fundamentals of the Design 21
3.2 ATHENA Model 25
3.2.1 Core Analysis Radial Rings 25
3.2.2 Core Unit Cell Representation 26
3.2.3 Core Materials 26
3.2.4 Hydraulic Nodalization 27
3.2.5 Conduction and Radiation Circuits 28
3.2.6 Model Specifications 29
3.2.7 Steady State Analysis 30
3.3 Simulated LOCA Analysis 31
3.3.1 Evolution of the ATHENA Model 31
3.3.1.1 Heat Transfer Correlations 31
3.3.1.2 Influence of Guard Containment Back Pressure 34
3.3.1.3 Water Decay Heat Removal Loop 34
3.3.1.4 Radial Peaking Factor 39
3.3.1.5 SiC Thermal Conductivity Investigation 41
3.3.1.6 Containment – RCCS Interface Modeling 41
3.4 Conclusions 41

1. Executive Summary

The Idaho National Laboratory (INL) contribution to the Nuclear Energy Research Initiative (NERI) project number 2002-005 was divided into reactor physics, and thermal-hydraulics and plant design. The research targeted credible physics and thermal-hydraulics models for a gas-cooled fast reactor, analyzing various fuel and in-core fuel cycle options to achieve a true breed and burn core, and performing a design basis Loss of Coolant Accident (LOCA) analysis on that design.

For the physics analysis, a 1/8 core model was created using different enrichments and simulated equilibrium fuel loadings. The model was used to locate the hot spot of the reactor, and the peak to average energy deposition at that location. The model was also used to create contour plots of the flux and energy deposition over the volume of the reactor. The eigenvalue over time was evaluated using three different fuel configurations with the same core geometry. The breeding capabilities of this configuration were excellent for a 7% U-235 model and good in both a plutonium model and a 14% U-235 model. Changing the fuel composition from the Pu fuel which provided about 78% U-238 for breeding to the 14% U-235 fuel with about 86% U-238 slowed the rate of decrease in the eigenvalue a noticeable amount. Switching to the 7% U-235 fuel with about 93% U-238 showed an increase in the eigenvalue over time.

For the thermal-hydraulic analysis, the reactor design used was the one forwarded by the MIT team. This reactor design uses helium coolant, a Brayton cycle, and has a thermal power of 600 MW. The core design parameters were supplied by MIT; however, the other key reactor components that were necessary for a plausible simulation of a LOCA were not defined. The thermal-hydraulic and plant design research concentrated on determining reasonable values for those undefined components.

The LOCA simulation was intended to provide insights on the influence of the Reactor Cavity Cooling System (RCCS), the containment building, and a Decay Heat Removal System (DHRS) on the natural circulation heat transfer of the core's decay heat. A baseline case for natural circulation had to be established in order to truly understand the impact of the added safety systems. This baseline case did not include a DHRS, although the current MIT design does have a DHRS that features the highly efficient Printed Circuit Heat Exchangers (PCHEs).

The initial LOCA analysis revealed that the RCCS was insufficient to maintain the reactor core below the fuel matrix decomposition temperature. A guard containment was added to the model in order to maintain a prescribed backpressure during the LOCA to enhance the natural circulation. The backpressure approach did provide satisfactory natural convection during the LOCA. The necessary backpressure was 1.8 MPa, which was not especially different from the values reported by other gas fast reactor researchers. However, as the model evolved to be more physically representative of a nuclear reactor, i.e., it included radial peaking factors, inlet plenum orificing, and the degradation of SiC thermal properties as a result of irradiation, the LOCA-induced fuel temperatures were not consistently below the decomposition limit.

2. Task A: Core Physics

A 1/8 core MCNP[1] model of the breed and burn reactor has been created. The model contains 990 cells in which the fuel is smeared with the other core materials (coolant, matrix material, etc.) The radius of the core is 124 cm with the reflector extending another 100 cm. The height of the core is 100 cm with a 100 cm thick reflector above and below the core.

The model was used to locate the hot spot of the reactor and the peak to average energy deposition at this location. This model was also used to create contour plots of the flux and energy deposition over the volume of the reactor. The eigenvalue over time was evaluated using three different fuel configurations with the same core geometry.

The model was also used to look at the breed and burn aspects of a variety of isotopes in different fuel configurations. The details of these analyses and the results are discussed here. Results have been presented previously for this reactor using a very low (unrealistic) power level for the depletion steps. This error has been corrected with the corrected data presented here.

2.1 Model Details

The model was created using the lattice fill method of MCNP. Each of the fuel cells is a right hexagonal prism 10 cm across the flats and 10 cm high. Each fuel cell is a unique universe with a unique material number. This provides the ability to deplete each fuel cell using the MOCUP[2] code (MCNP-ORIGEN2 Coupled Utility Program). The azimuthal boundaries are modeled as reflective surfaces to take advantage of symmetry and mimic a full core without extending the geometry and thus, the computer processing time required for the analysis. A Zr_3Si_2 reflector extends 100 cm beyond the active core radially and 100 cm above and below the core axially. The source was defined as a uniformly distributed source over the volume of the active core. Figures 1 and 2 present a radial cross section of the core at the mid plane and an axial cross section through the hotspot. Both figures include the cell numbers for referencing purposes later.

MOCUP uses tally information from MCNP to provide material composition, flux, and collapsed 1-group cross sections for ORIGEN2[3] depletion calculations. MOCUP calculates the necessary information and inserts it into the ORIGEN2 input file before initiating the ORIGEN2 run. The ORIGEN2 output is then used by MOCUP to calculate the new material composition for the depleted cell, generate a new material card, and then insert it into the next MCNP input file. MOCUP then runs MCNP with the new input file to calculate the new eigenvalue and new flux and cross sections. This process is performed for each depletion cell for each depletion step. The depletion cycles were set up to occur at 60 day increments for 24 cycles which is equal to about 3.9 years.

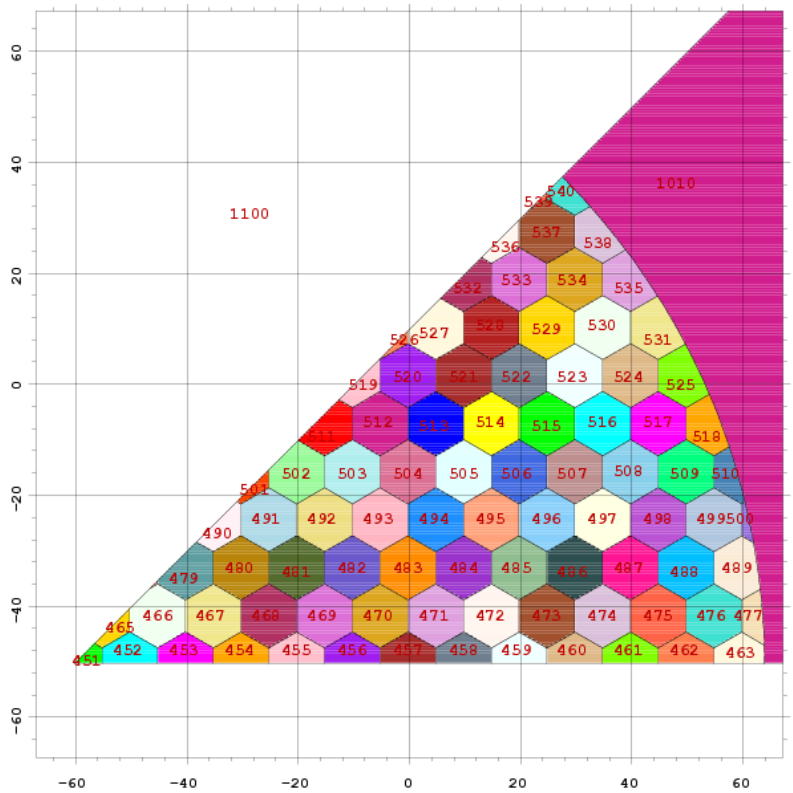

Figure 1: Radial cross section through the mid plane of the core showing the MCNP cell number

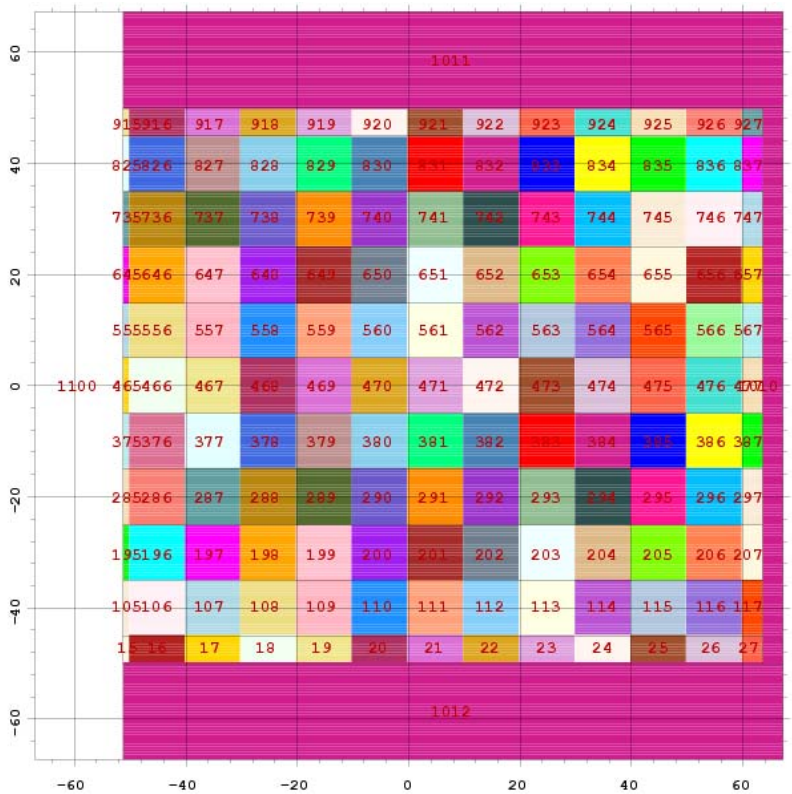

Figure 2: Axial cross section of the core through the hot spot showing the MCNP cell numbers.

This same geometric model was run with three different fuel compositions. The first was a uranium carbide fuel with 16 weight percent plutonium, 4 weight percent in major actinides (neptunium, americium, and curium), and the rest being natural uranium. The second and third fuel compositions contained no plutonium or major actinides, but were enriched to 14% U-235 and 7% U-235 respectively. The plutonium-fueled model at BOL was used to determine the location of the hot spot and to calculate the peak to average ratio for this location. It was also used to evaluate the neutron spectrum, and generate contour plots of the energy and neutron flux. A cylindrical mesh tally was set up for MCNPX[4] to provide the data for the contour plot. The MCNPX plotting feature was used to generate the contour plots.

2.2 Neutronics Results

From the BOL Pu fueled model, a variety of important neutronics information was generated for this core configuration. A tally in each cell determined that the hot spot of the core occurs in cell 467 with the peak to average at that location being 2.3. Figure 3 shows a neutron flux spectrum for the hot spot of the core and average over the active core. As is expected, the spectrum is consistent with a fast reactor spectrum.

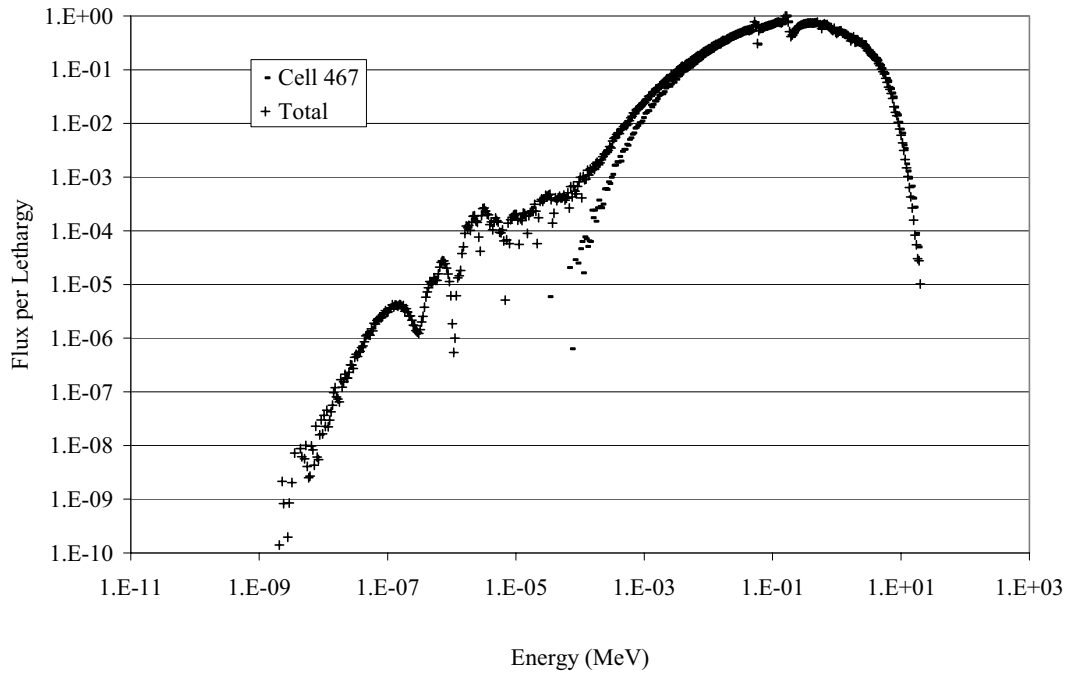

Figure 3: Plot of the flux per lethargy for cell 467 which is the location of the hot spot of the core, and the average spectrum over the whole active core.

Figures 4 through 7 show contour plots for the radial flux profile, the axial flux profile, the radial total energy deposition profile, and the axial total energy profile respectively.

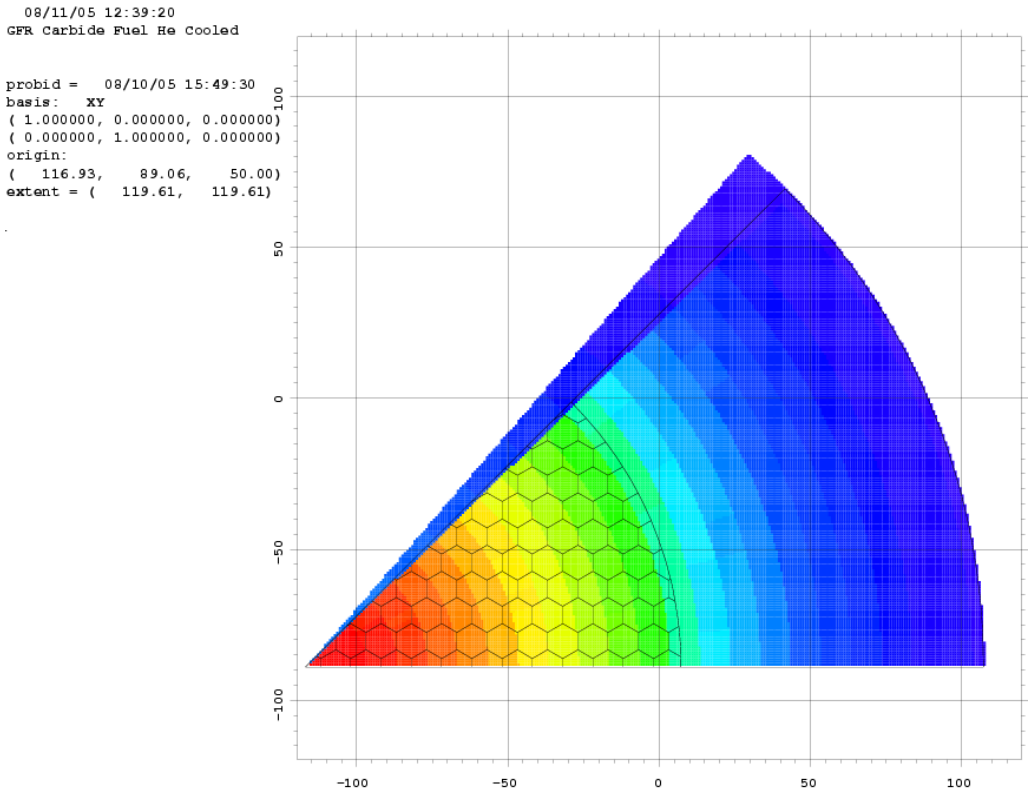

Figure 4: Radial Flux profile at the mid-plane of the core.

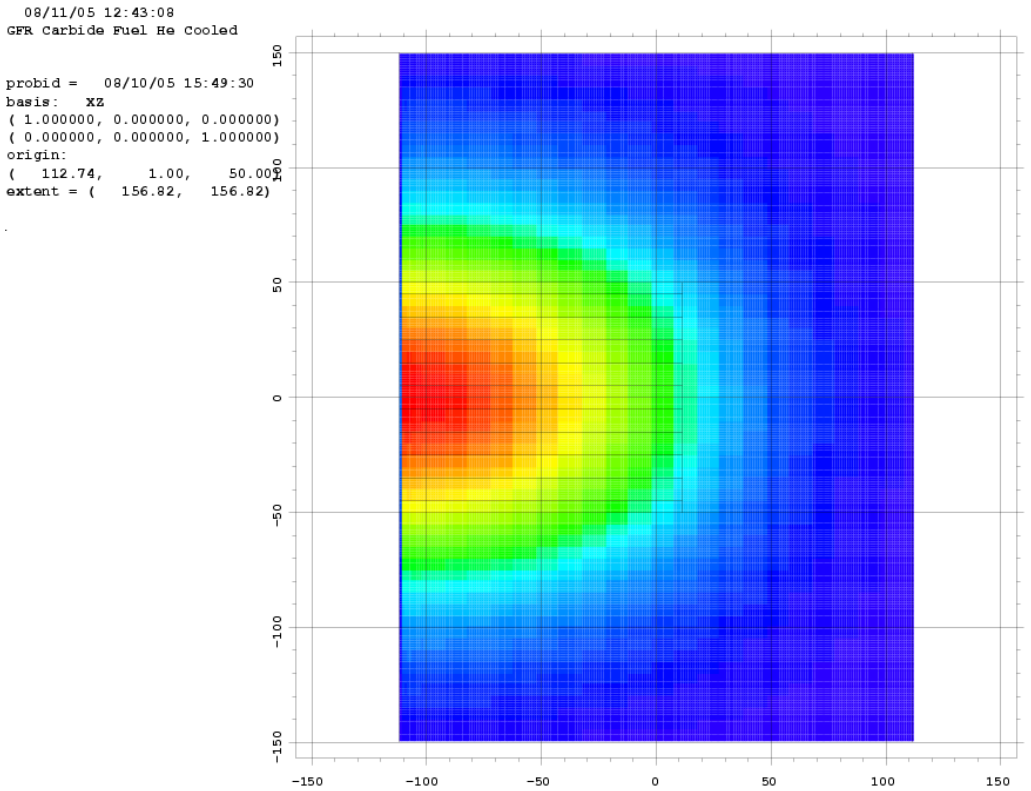

Figure 5: Axial flux profile through the center of the core.

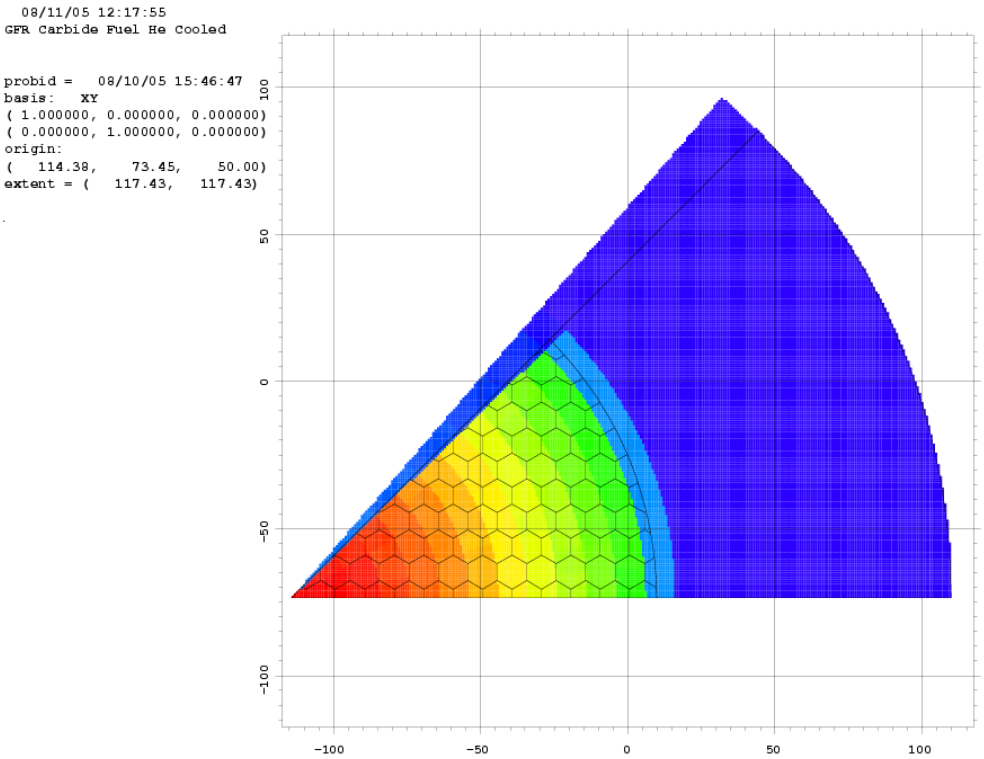

Figure 6: Radial heating profile at the mid-plane of the core.

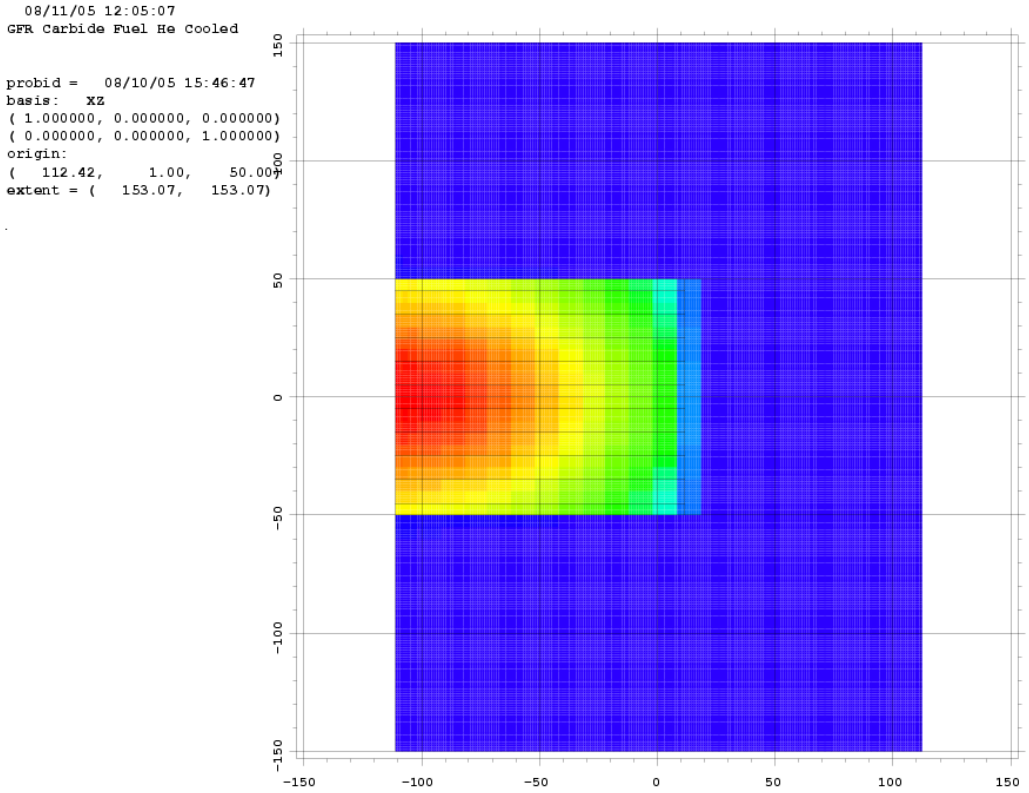

Figure 7: Axial heating profile through he center of the core.

The combination of the limited color resolution for the MCNPX contour plots combined with the difference in the energy deposition rate in the active core as compared to the reflector (about two orders of magnitude) results in the reflector in the contour plot being represented as one color.

The neutronics data presented in the previous figures is what you would expect from this configuration, and is an indication that this model is representative of the configuration.

2.3 Plutonium Fueled Depletion Model

As mentioned previously, MOCUP was used to couple MCNP and ORIGEN2 to estimate the effects of fuel burn-up over several years worth of run time. The reactor specifications for the Pu fueled depletion model are presented in Table 1. The dimensions presented in the table are for the complete core geometry and not the 1/8 core model. The volume and power of the 1/8 model is 0.604 m^3 and 60.4 MW respectively.

The effect of fuel burn-up on the eigenvalue of the reactor is presented in Figure 8. The decrease in the eigenvalue is approximately 0.027Δk (1.183 to 1.156) in four years. Four years corresponds to about 38 MWd/kg of heavy metal. The change in the individual fuel isotopes is best viewed in graphical form. The isotopes of uranium, neptunium, plutonium, americium, and curium are displayed in Figures 9 through 13.

The uranium isotopes and the Np-237 isotope show a significant depletion over the time period evaluated. Pu-239 and Pu-241 deplete gradually over the time period while Pu-238 and Pu-242 show an increase. The concentration of Pu-240 stays relatively constant. Am-241, Am-242, and Am-243 deplete gradually over the time period. Am-242m increases over time and approaches a steady state concentration. Cm-244 gradually increases over time while Cm-242 and Cm-243 approach a steady state concentration.

Table 1: Plutonium fueled Gas-Cooled Fast Reactor specifications.

Overall Core Specifications	
Power Density	100 W/cm^3
Height	1 m
Radius	1.24 m
Volume	4.83 m^3
Total Power	483 MW
Coolant Specifications	
Coolant	He
System Pressure	7 MPa
Coolant Volume Fraction	40%
Fuel Block Specifications	
Shape	Hexagonal prism
Height	10 cm
Dimension across flats	10 cm
Quantity	990
Fuel + Matrix Volume Fraction	60%
Fuel	UC
Matrix Material	SiC
Fuel to Matrix Ratio	50%
Fuel Constituents	
Natural Uranium	78.94%
Pu	16.85%
Pu-238	0.33%
Pu-239	9.75%
Pu-240	4.39%
Pu-241	1.69%
Pu-242	0.68%
Minor Actinides	4.21%
Np-237	1.81%
Am-241	1.89%
Am-243	0.38%
Cm-244	0.13%
Reflector Specifications	
Reflector Material	Zr_3Si_2
Axial Thickness	1 m
Radial Thickness	1 m

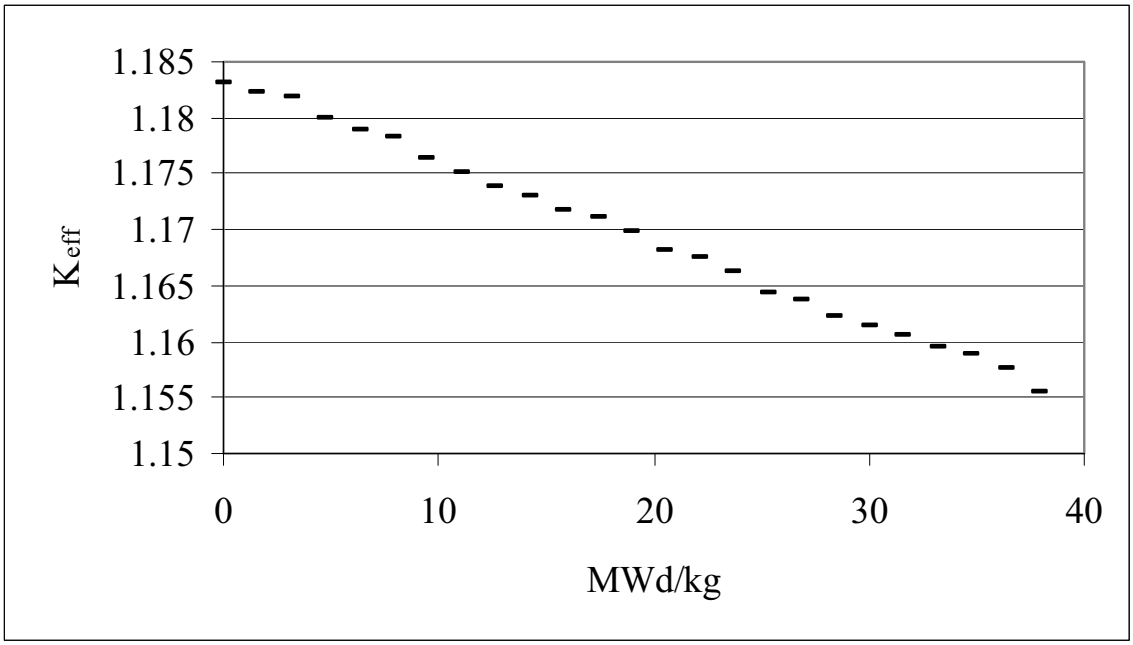

Figure 8: Change in K_{eff} vs. burn-up in the plutonium fueled model.

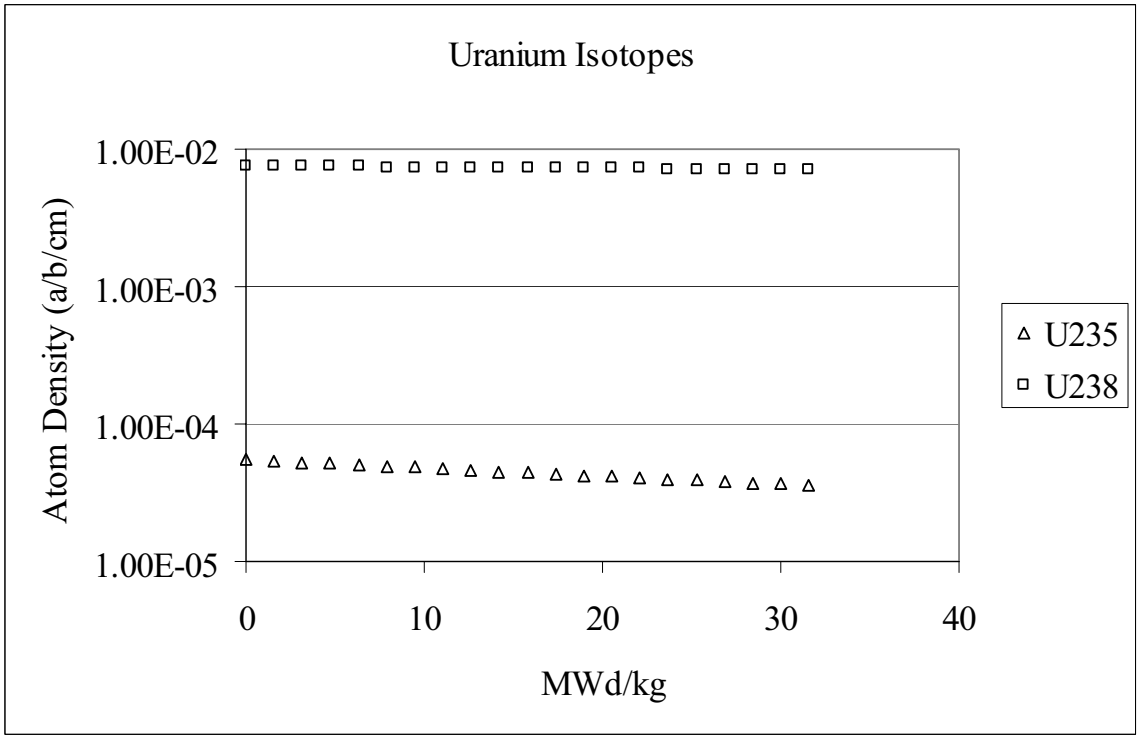

Figure 9: Change in the uranium composition of the fuel vs. burn-up in the plutonium fueled model.

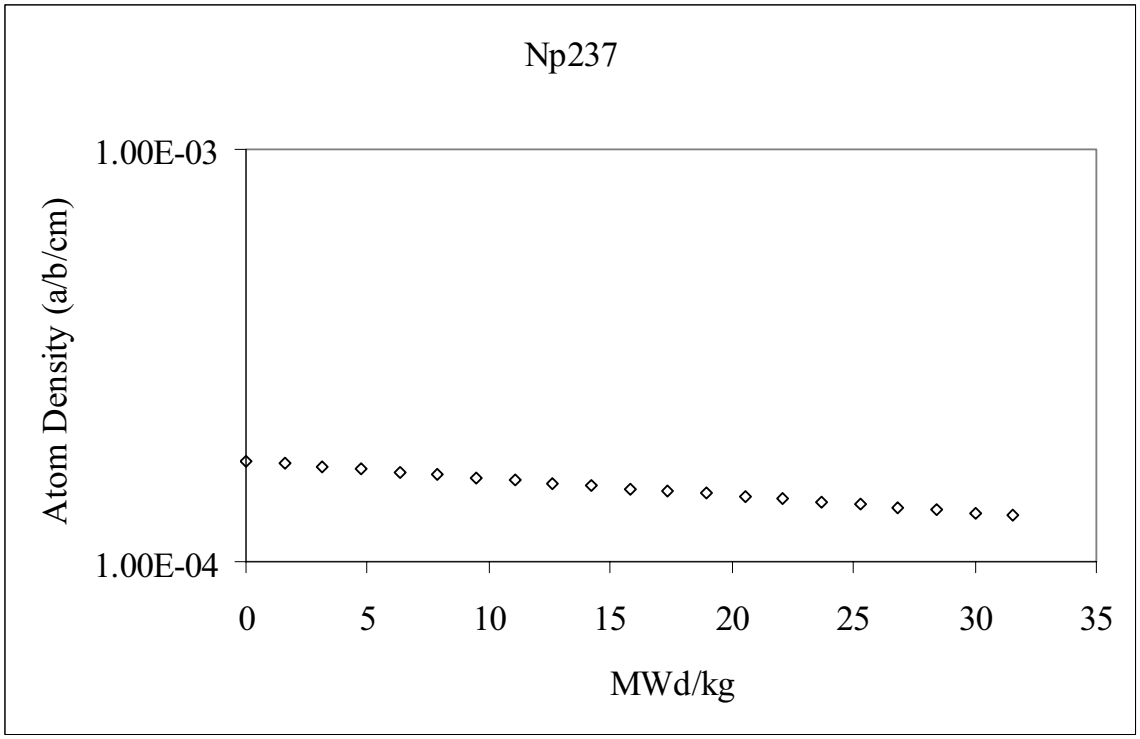

Figure 10: Change in the neptunium composition of the fuel vs. burn-up in the plutonium fueled model.

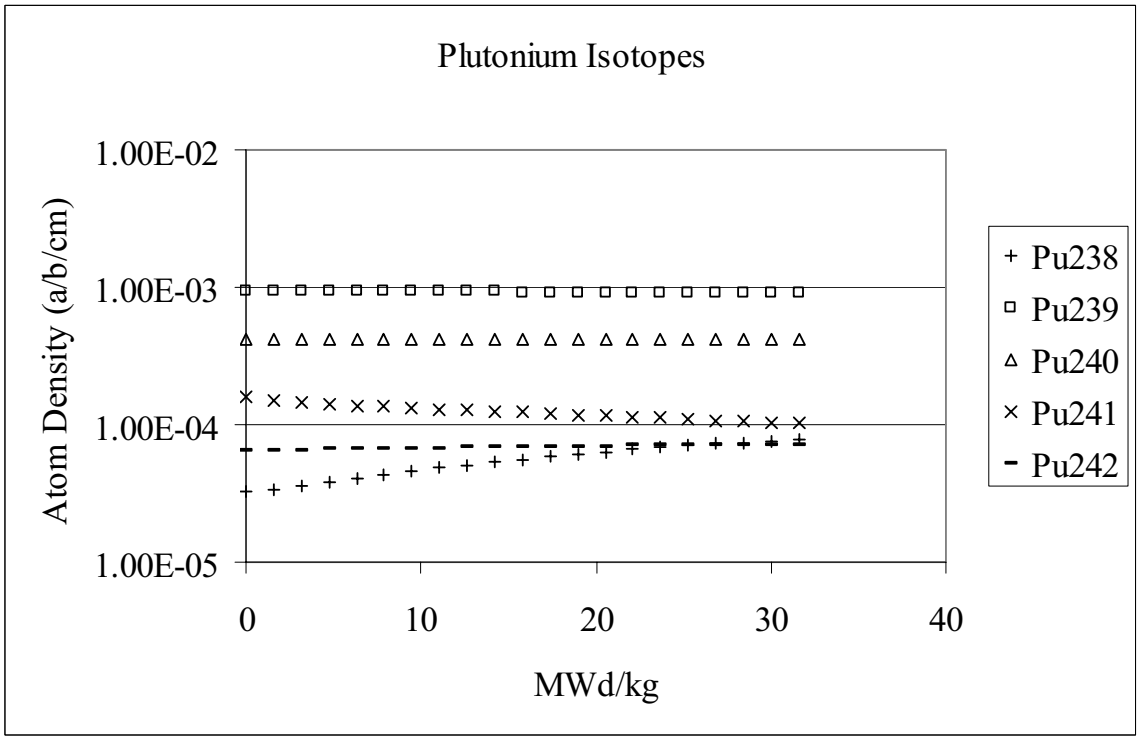

Figure 11: Change in the plutonium composition of the fuel vs. burn-up in the plutonium fueled model.

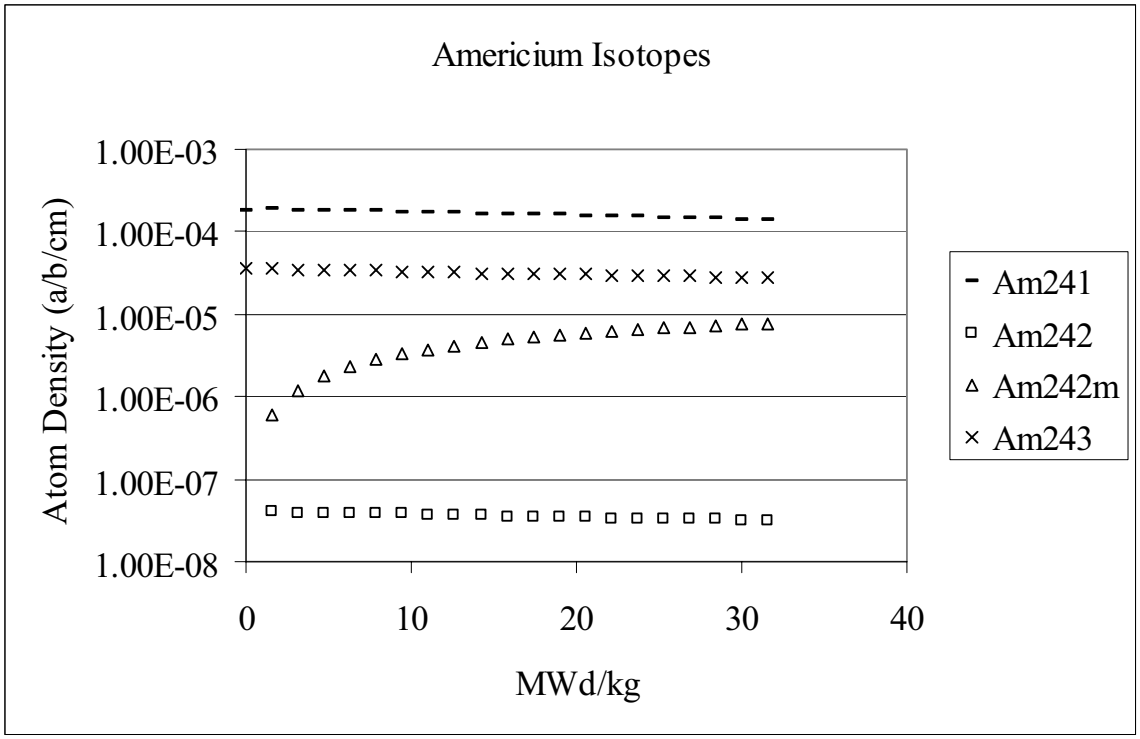

Figure 12: Change in the americium composition of the fuel vs. burn-up in the plutonium fueled model.

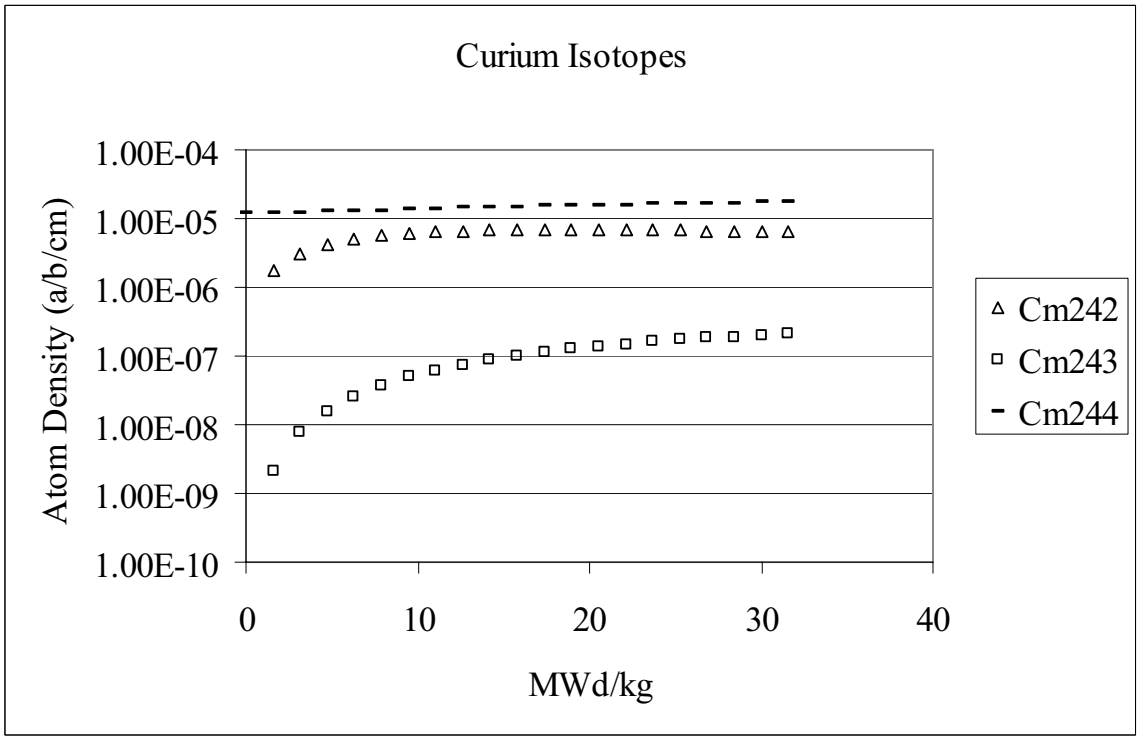

Figure 13: Change in the curium composition of the fuel vs. burn-up in the plutonium fueled model.

2.4 14% Enriched Uranium Fueled Depletion Model

The reactor specifications for the 14% U-235 fueled depletion model are presented in Table 2. The effect of fuel burn-up on the eigenvalue of the reactor is presented in Figure 14. The decrease in the eigenvalue is approximately 0.016 Δk (1.054 to 1.038) in four years. The isotopes of uranium, neptunium, plutonium, americium, and curium are displayed in Figures 15 through 19.

The uranium isotopes deplete over time with U-235 showing a significant depletion. All of the other isotopes (Np-237, Pu-238, Pu-239, Pu-240, Pu-241, Pu-242, Am-241, Am-242, Am-242m, Am-243, Cm-242, Cm-243, and Cm244) increase over time and approach a steady state concentration.

Table 2: 14% U-235 fueled Gas-Cooled Fast Reactor specifications.

Overall Core Specifications	
Power Density	100 W/cm^3
Height	1 m
Radius	1.24 m
Volume	4.83 m^3
Total Power	483 MW
Coolant Specifications	
Coolant	He
System Pressure	7 MPa
Coolant Volume Fraction	40%
Fuel Block Specifications	
Shape	Hexagonal prism
Height	10 cm
Dimension across flats	10 cm
Quantity	990
Fuel + Matrix Volume Fraction	60%
Fuel	UC
Matrix Material	SiC
Fuel to Matrix Ratio	50%
Fuel Constituents	
U-234	0.01%
U-235	13.85%
U-238	86.15%
Reflector Specifications	
Reflector Material	Zr_3Si_2
Axial Thickness	1 m
Radial Thickness	1 m

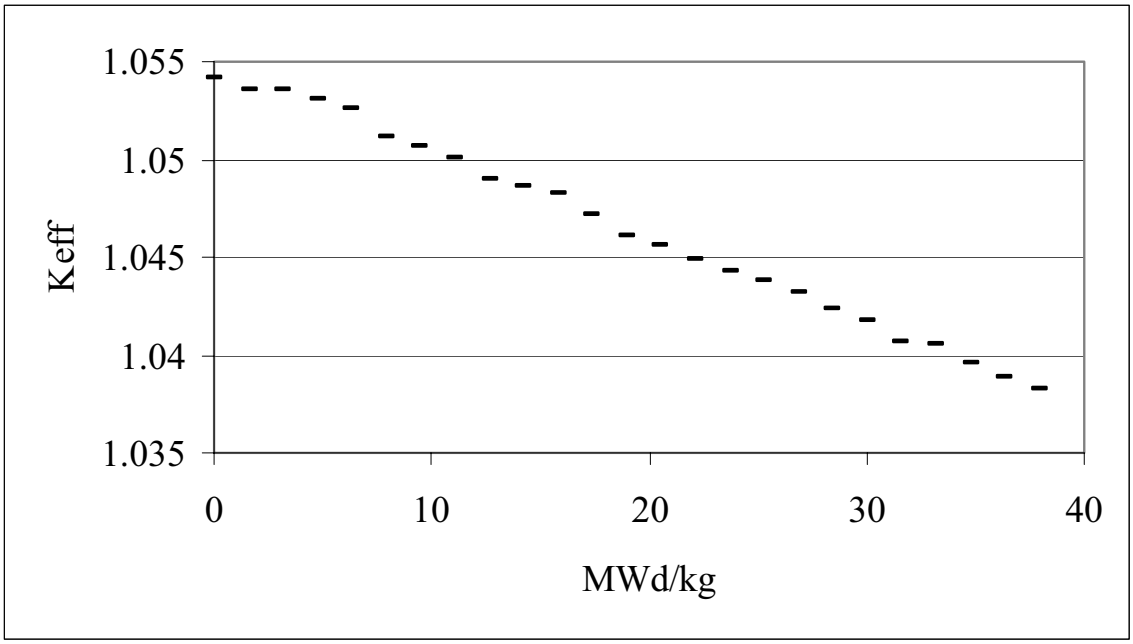

Figure 14: Change in K_{eff} vs. burn-up in the 14% U-235 fueled model.

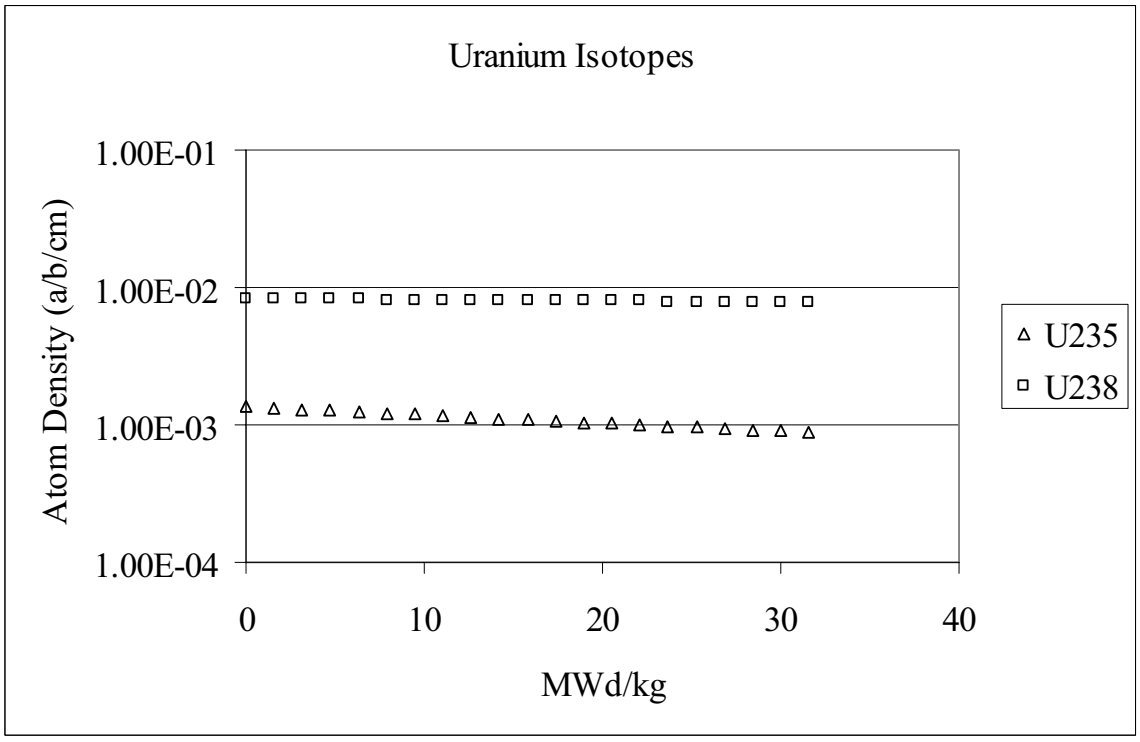

Figure 15: Change in the uranium composition of the fuel vs. burn-up in the 14% U-235 fueled model.

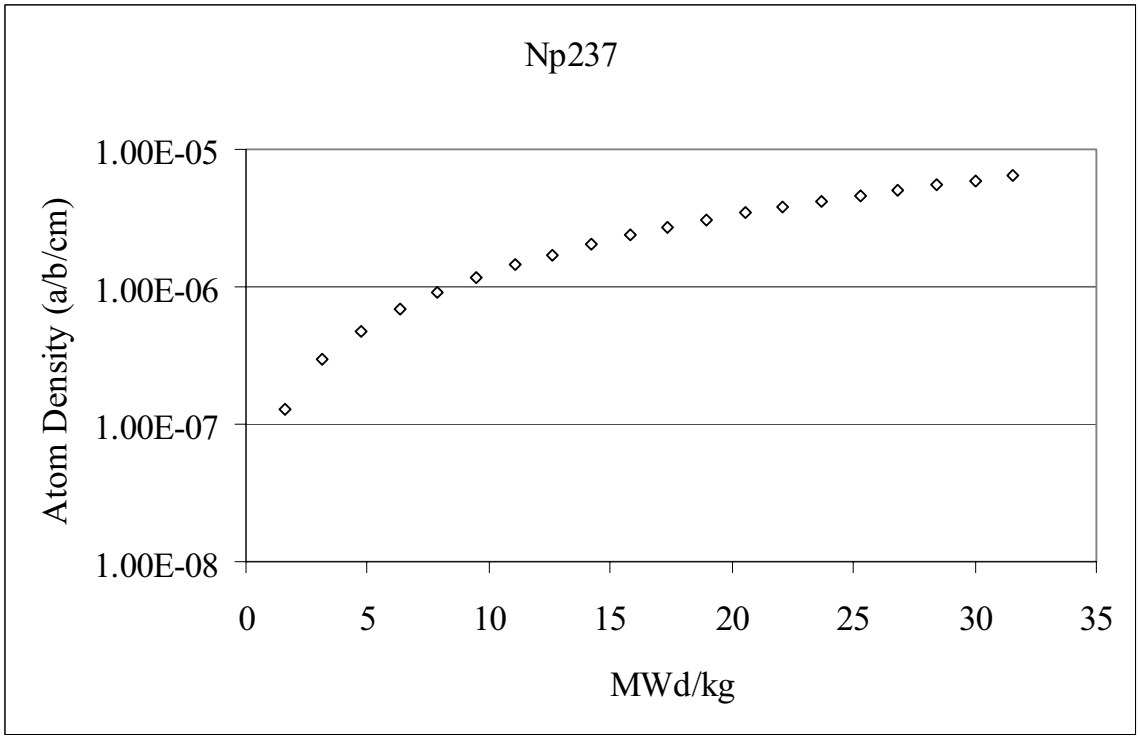

Figure 16: Change in the neptunium composition of the fuel vs. burn-up in the 14% U-235 fueled model.

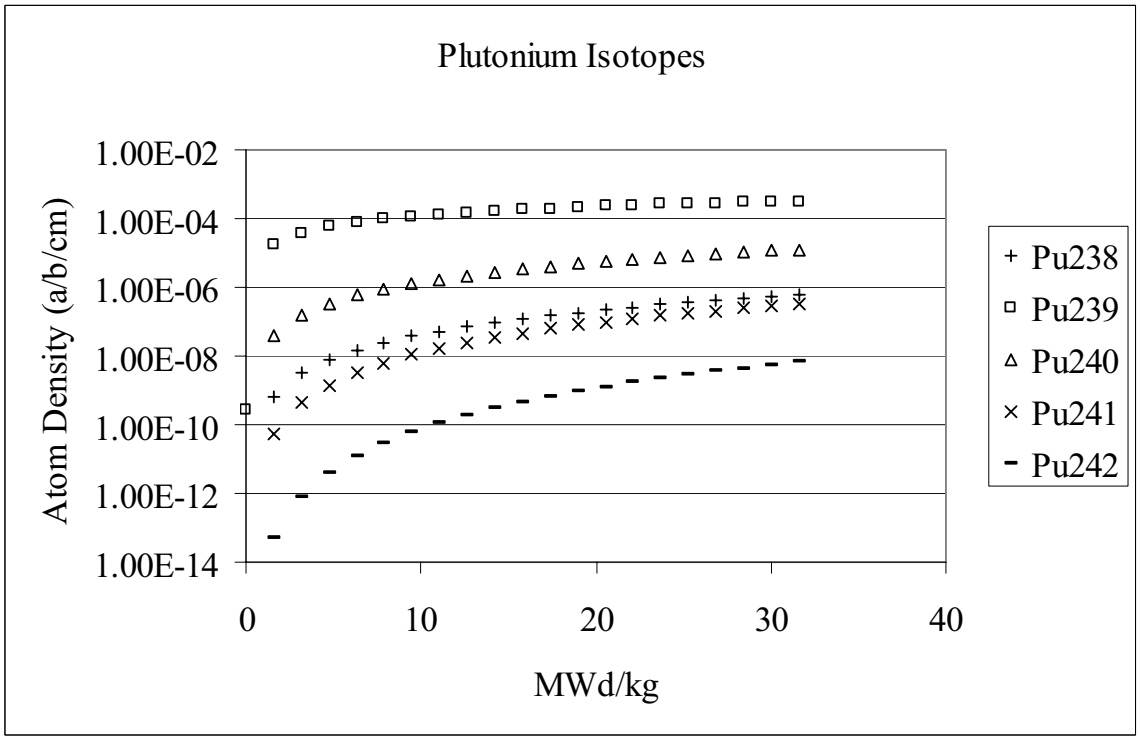

Figure 17: Change in the plutonium composition of the fuel vs. burn-up in the 14% U-235 fueled model.

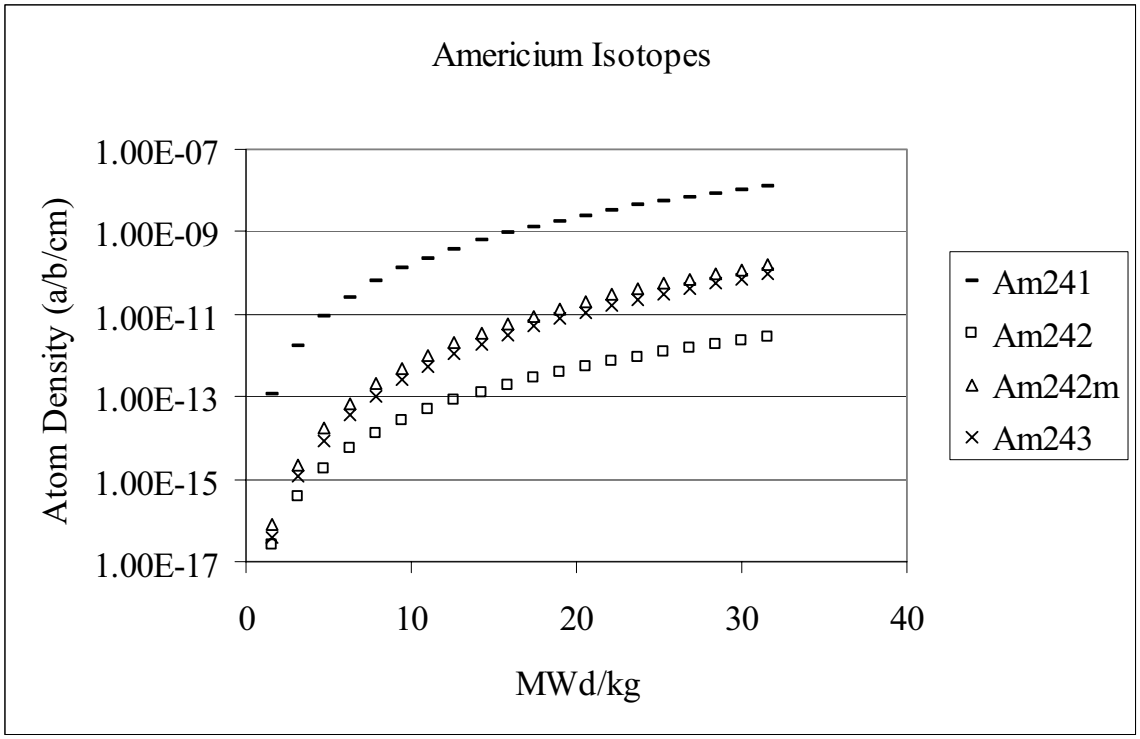

Figure 18: Change in the americium composition of the fuel vs. burn-up in the 14% U-235 fueled model.

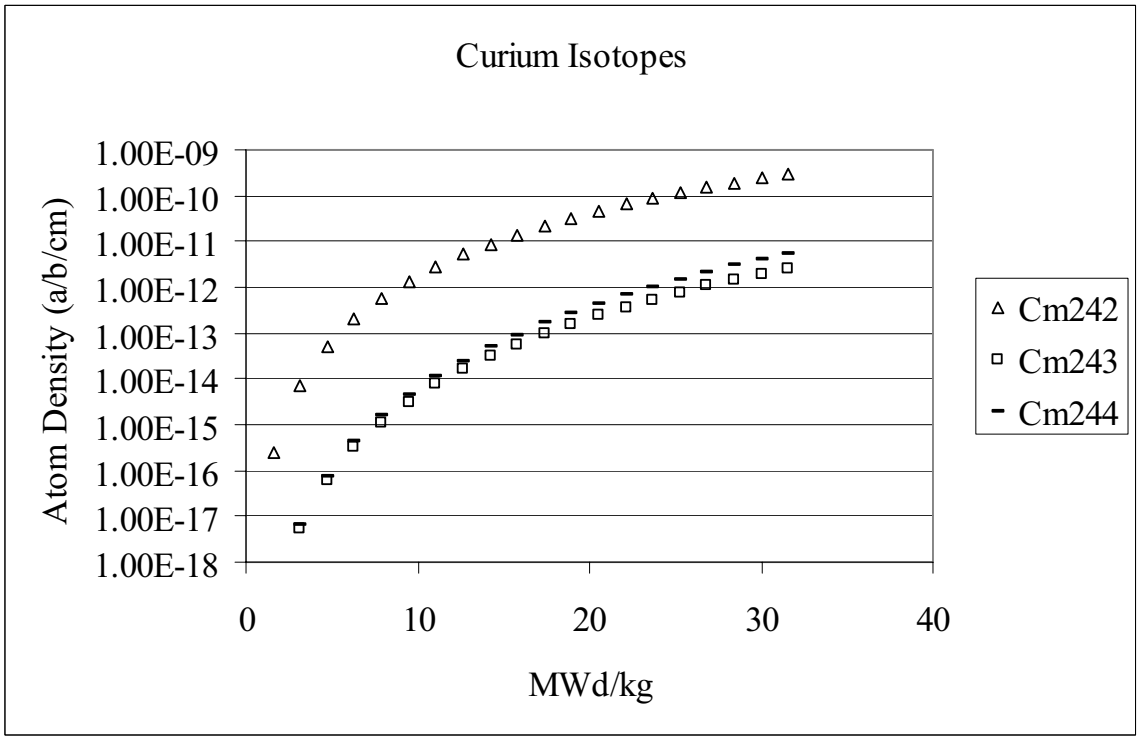

Figure 19: Change in the curium composition of the fuel vs. burn-up in the 14% U-235 fueled model.

2.5 7% Enriched Uranium Fueled Depletion Model

The reactor specifications for the 14% U-235 fueled depletion model are presented in Table 3. The effect of fuel burn-up on the eigenvalue of the reactor is presented in Figure 20. The increase in the eigenvalue is approximately 0.117 Δk (0.753 to 0.870) in four years. The isotopes of uranium, neptunium, plutonium, americium, and curium are displayed in Figures 21 through 25.

As with the 14% U-235 model, the uranium isotopes deplete over time with U-235 showing a significant depletion. All of the other isotopes (Np-237, Pu-238, Pu-239, Pu-240, Pu-241, Pu-242, Am-241, Am-242, Am-242m, Am-243, Cm-242, Cm-243, and Cm244) increase over time and approach a steady state concentration.

Table 3: 7% U-235 fueled Gas-Cooled Fast Reactor specifications.

Overall Core Specifications	
Power Density	100 W/cm^3
Height	1 m
Radius	1.24 m
Volume	4.83 m^3
Total Power	483 MW
Coolant Specifications	
Coolant	He
System Pressure	7 MPa
Coolant Volume Fraction	40%
Fuel Block Specifications	
Shape	Hexagonal prism
Height	10 cm
Dimension across flats	10 cm
Quantity	990
Fuel + Matrix Volume Fraction	60%
Fuel	UC
Matrix Material	SiC
Fuel to Matrix Ratio	50%
Fuel Constituents	
U-234	0.01%
U-235	6.92%
U-238	93.08%
Reflector Specifications	
Reflector Material	Zr_3Si_2
Axial Thickness	1 m
Radial Thickness	1 m

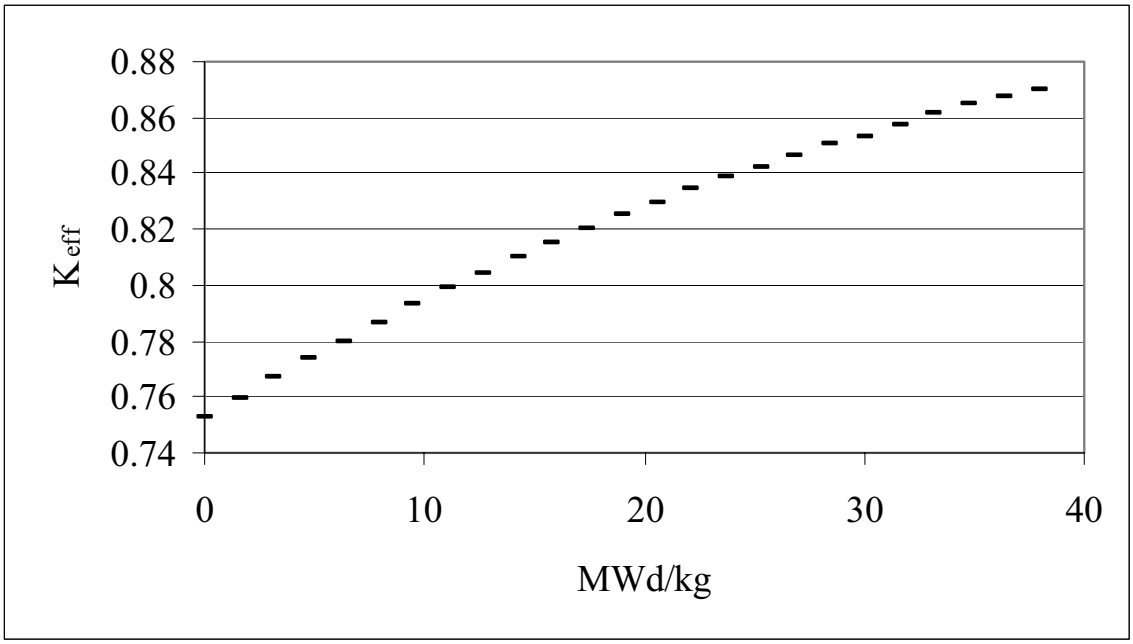

Figure 20: Change in K_{eff} vs. burn-up in the 7% U-235 fueled model.

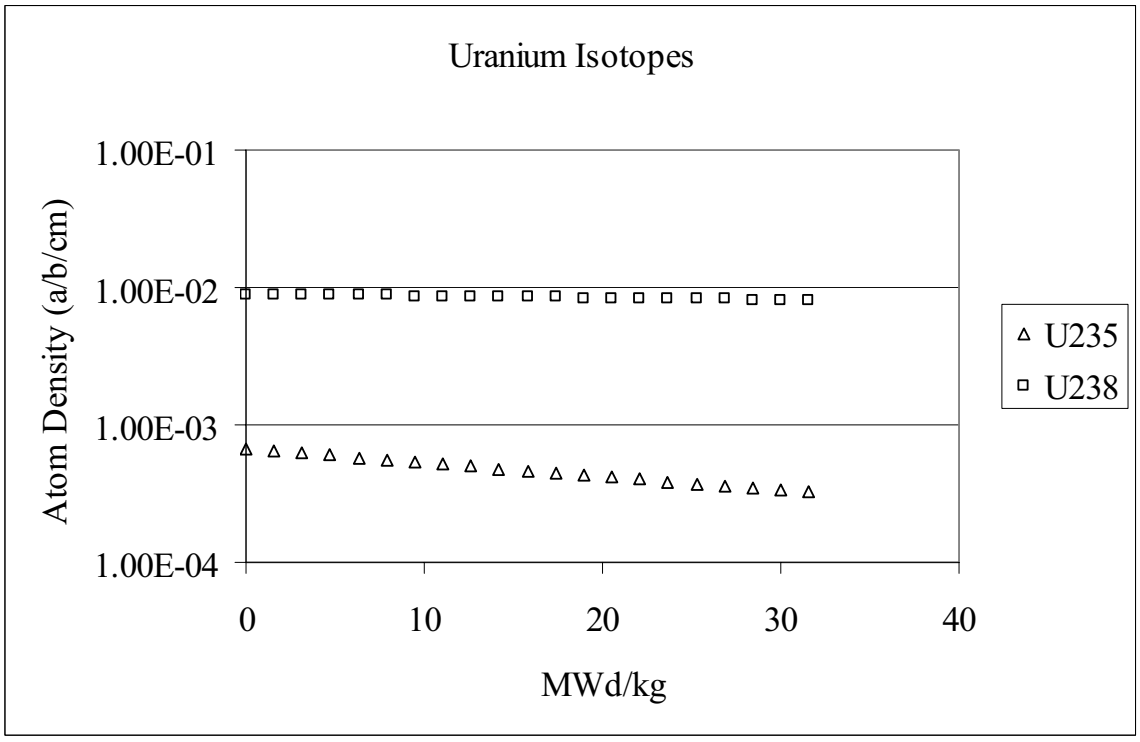

Figure 21: Change in the uranium composition of the fuel vs. burn-up in the 7% U-235 fueled model.

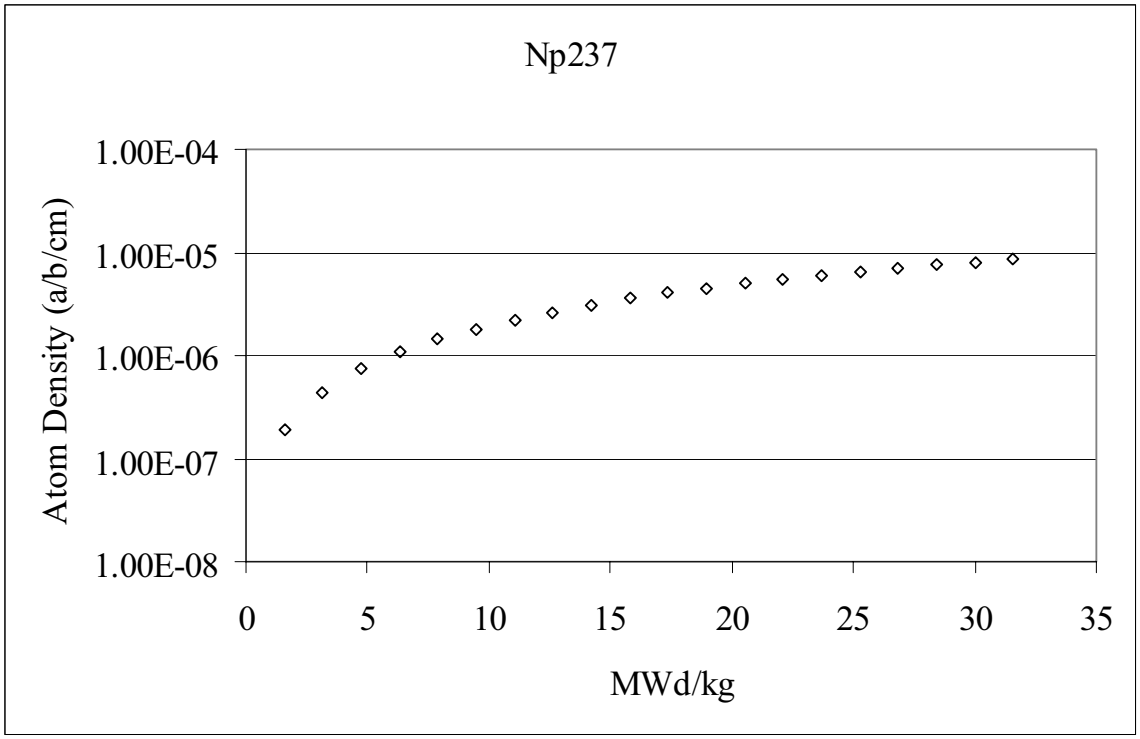

Figure 22: Change in the neptunium composition of the fuel vs. burn-up in the 7% U-235 fueled model.

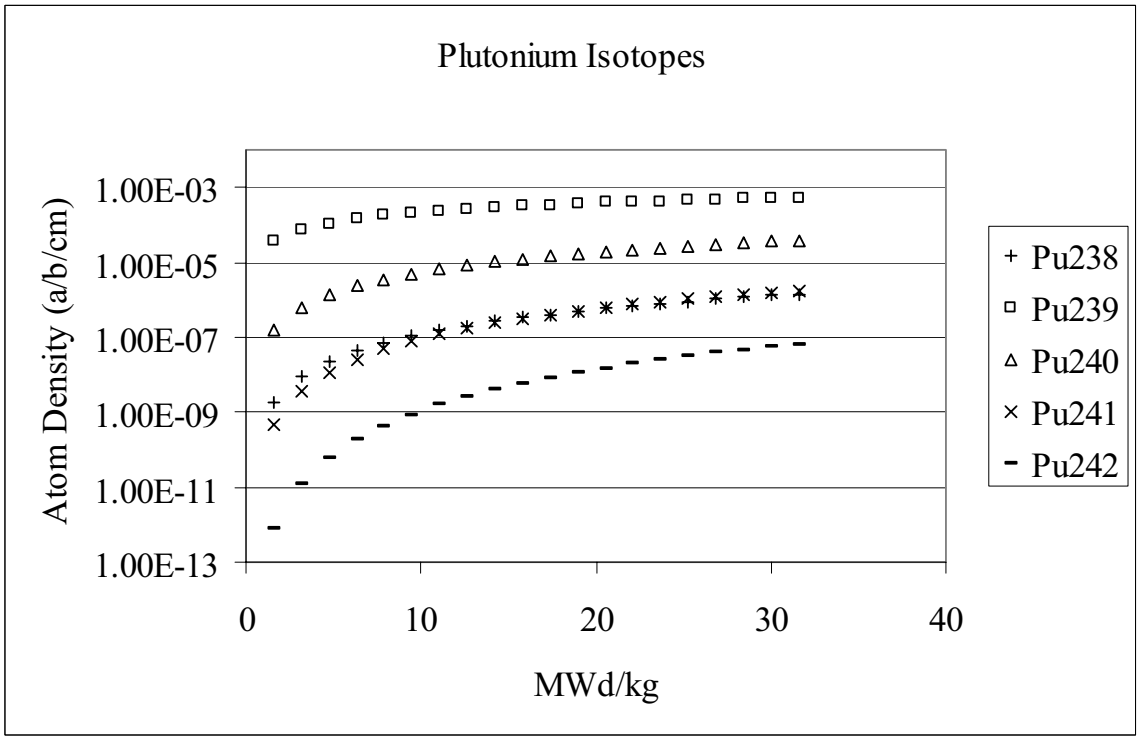

Figure 23: Change in the plutonium composition of the fuel vs. burn-up in the 7% U-235 fueled model.

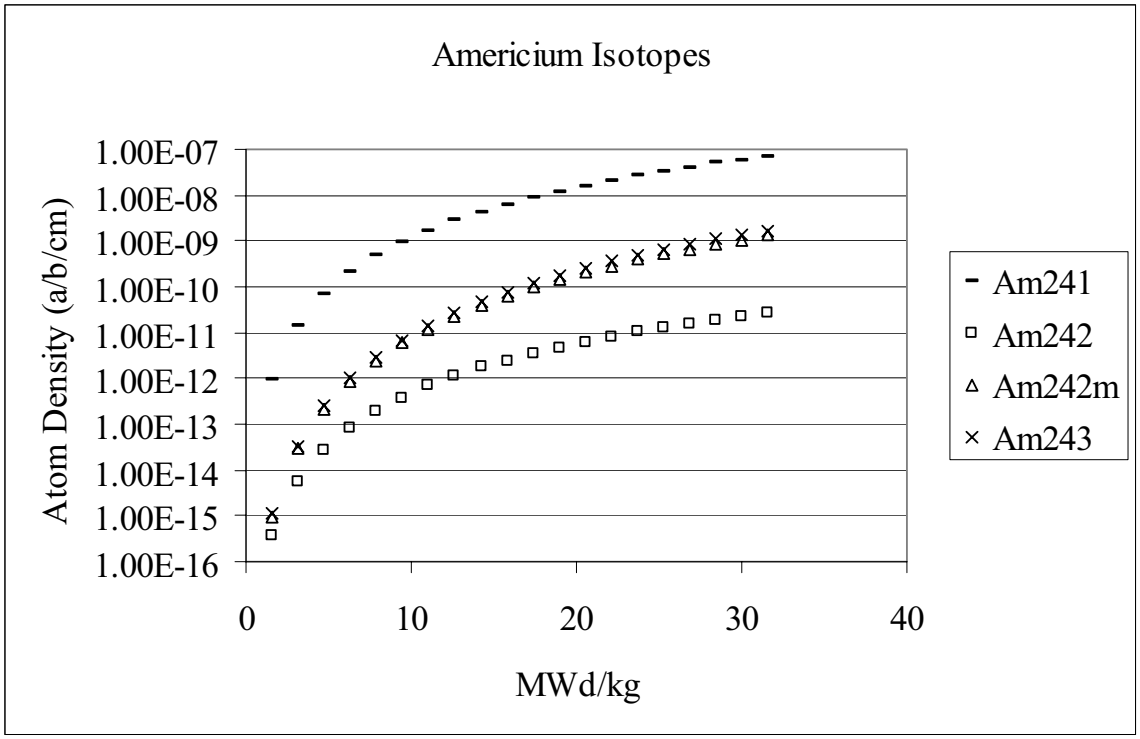

Figure 24: Change in the americium composition of the fuel vs. burn-up in the 7% U-235 fueled model.

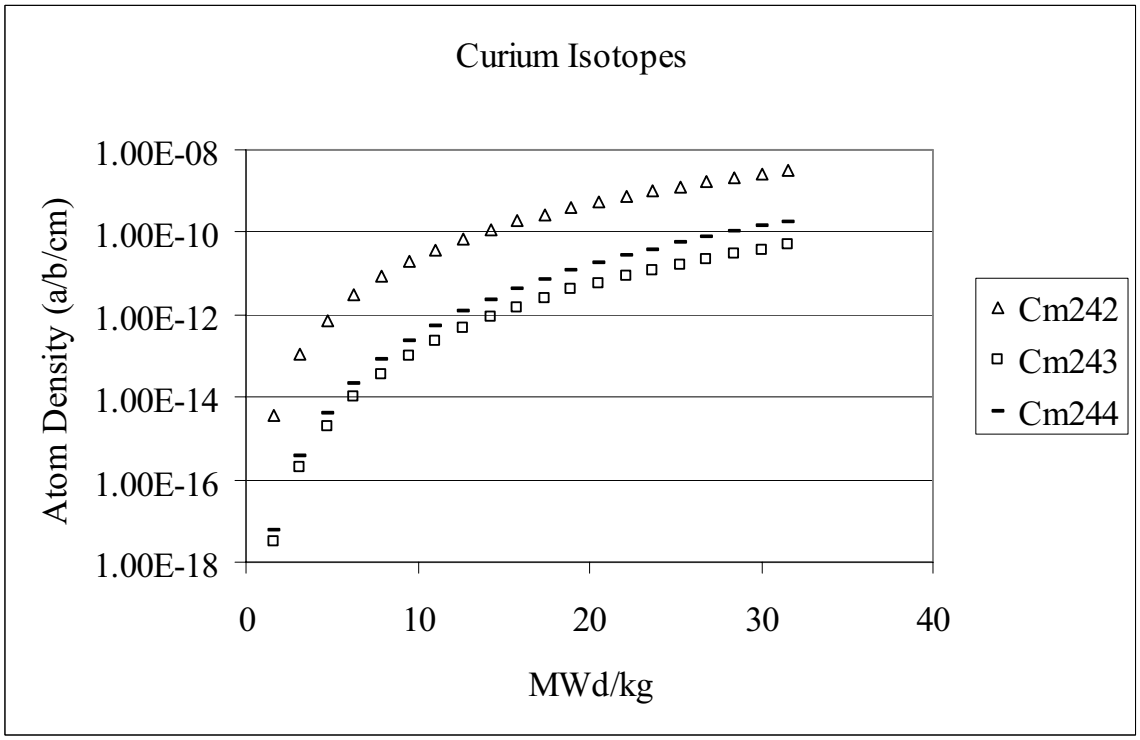

Figure 25: Change in the curium composition of the fuel vs. burn-up in the 7% U-235 fueled model.

2.6 Conclusions

The breeding capabilities of this configuration are obvious in the 7% U-235 model and evident in both the plutonium model and the 14% U-235 model. Changing the fuel composition from the Pu fuel which provided about 78% U-238 for breeding to the 14% U-235 fuel with about 86% U-238 slowed the rate of decrease in the eigenvalue a noticeable amount. Switching to the 7% U-235 fuel with about 93% U-238 showed an increase in the eigenvalue over time. The proper proportioning of U-238 to fissile material may provide a reactor with an eigenvalue that doesn't change or changes minimally over time.

Further studies to focus in on an optimal loading could include iterating on different fuel mixtures to locate the optimal mixture for a uniformly loaded core. Varying fuel mixtures in the core in zones to provide optimal usage of the neutrons in each zone and possibly decreasing the peak to average heat rate. This may provide a more uniform flux over the core and more efficient use of all the fuel in the core. Studies could also be conducted on moving fuel around the core based on its burn-up to provide zone loading of the reactor through time to again provide better use of the fuel and the neutrons in the reactor.

3. Tasks B and C: Core Thermal Hydraulics and Plant Design

The goal of this research was to examine gas fast reactor thermal response during a severe off-normal scenario in which reactor decay heat is removed solely by a passive method. The off-normal scenario selected for the analysis was a simultaneous and complete double guillotine break of the primary coolant inlet and outlet ducts.

The following sections discuss an effort to create a plausible thermal hydraulics model of a prototypical gas fast reactor and perform a Loss of Coolant Analysis (LOCA), which is a Nuclear Regulatory Commission design basis accident for nuclear reactor power plants. A discussion of the thermal hydraulics analysis code is provided, along with the modeling assumptions.

3.1 Fundamentals of the Design

The gas fast reactor design features a "pancake" style core (height/diameter ~ 1.7/2.9 m) that produces 600 MW of thermal power and has an average power density of 55 MW/m^3. The power density is a specific point of mentioning since this value affects economics, sustainability, and safety. Economics and sustainability requirements suggest high values of power density, while safety requirements suggest the opposite.

Helium is a benign coolant choice because it has small void reactivity feedback effects, and is not subject to any change of phase. However, the hard neutron spectrum makes the VHTR TRISO fuel technology unacceptable for gas fast reactor use: i.e., the fuel density is too low, and there is poor irradiation behavior of the pyrocarbon at high dose levels. For the gas fast reactor, a refractory matrix dispersion fuel of CERCER (ceramic fuel in a ceramic matrix) appears to provide the best combination of conductivity and high temperature performance.

In the reference design, the fuel configuration is based on dispersed fuel as particles in an inert plate/block type matrix. Uranium carbide is the reference fuel, as a result of its high heavy metal density, high thermal conductivity, and anticipated minimal impact on the neutron spectrum. Unlike TRISO fuel, the gas fast reactor particle fuel will have to maximize the heavy metal content within the matrix. The matrix/cladding material is SiC ceramic for its high temperature properties. Figure 26 shows the prismatic plate with coolant channels within the dispersed CERCER fuel matrix, while Figure 27 presents a cutaway illustration of fuel particles in a matrix configuration.

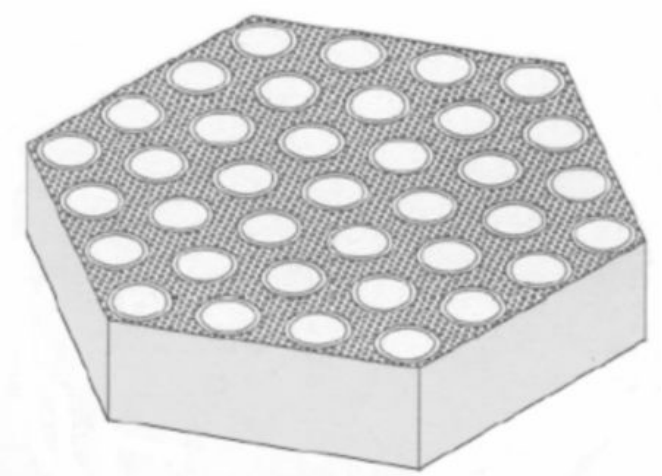

Figure 26: Schematic of a prismatic plate with dispersed fuel and coolant channels.

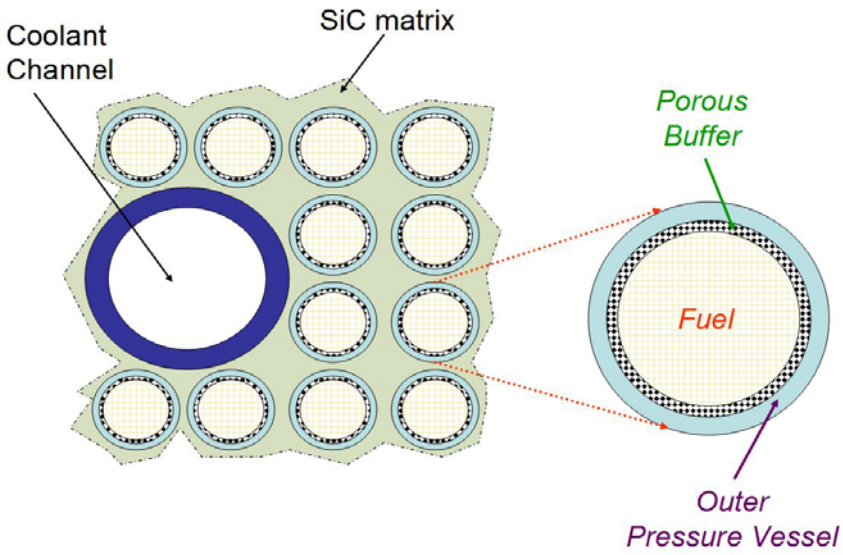

Figure 27: Cutaway of dispersed fuel plate, illustrating the components of the fuel particles and the particles placement within the fuel plate.

The reactor core in the reference design has a volume of 11 m^3 and reflectors envelop the core and neutron shields in both the radial and axial directions, refer to Figure 28. The reference coolant is Helium at an outlet pressure and temperature of 7 MPa and 850 °C, respectively. It is important to note in Figure 3 that the coolant flow path is upwards through the core.

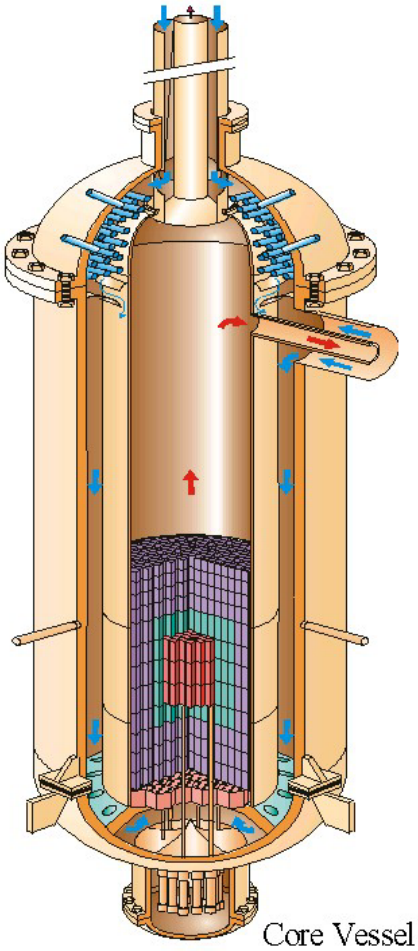

Figure 28: Prototypical reactor vessel configuration for the gas fast reactor.

The gas fast reactor has published typical operating parameters, as are presented in Table 4.

Table 4: Design Features for the gas fast reactor concept

Reactor Design Parameter	Conceptual Data
Power plant	600 MW_{th}
Net efficiency	48% (Helium, direct cycle)
Coolant pressure	9 MPa
Outlet coolant temperature	850 °C (Helium, direct cycle)
Inlet coolant temperature	490 °C (Helium, direct cycle)
Nominal flow and velocity	330 kg/s and 40 m/s
Core volume	10.9 m^3 (H/D ~1.7/2.9 m)
Core pressure drop	~ 0.04 MPa
Volume fraction (%) Fuel/Gas/SiC	50/40/10
Average power density	55 MW/m^3
Reference fuel compound	(U, Pu)C/SiC (50/50%) 17% Pu
Breeding/Burning performances	Self-Breeder
Maximum fuel temperature	1174 °C (normal operation) < 1650 °C (depressurization)
In core heavy nuclei inventory	30 tons
Fission rate (at %); Damage	~ 5 at%; 60 dpa
Fuel management	multi-recycling
Fuel residence time	3 x 829 efpd
Doppler effect (180 °C–1200 °C)	-1540×10^{-5}
Delayed neutron fraction	356×10^{-5}
Total He void effect	$+230 \times 10^{-5}$
Average burn-up rate at EOL	~ 5% FIMA
Primary vessel diameter	< 7 m

MIT used the information in Table 4 in conjunction with their neutronic and thermal hydraulic analyses to create a core configuration using dispersed fuel in prismatic blocks. The MIT core for the reference design has 127 prismatic blocks with 91 coolant holes per block, and a width of 20 cm for each hexagonal block. An illustration of the core and its fuel blocks is shown in Figure 29.

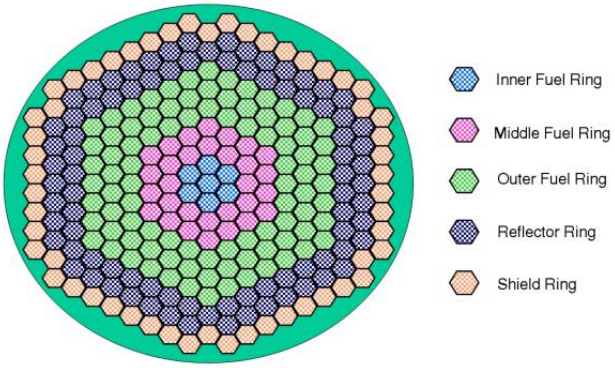

Figure 29: Illustration of the MIT core configuration for the reference design. The five radial "rings" used for creating the ATHENA model are also identified.

3.2 ATHENA Model

The thermal hydraulics code used to analyze the model and the simulated LOCA was the Reactor Excursion and Leak Analysis Program - 3 Dimensional (RELAP5-3D). RELAP5 was developed at the Idaho National Laboratory to allow the U.S. Nuclear Regulatory Commission to analyze postulated accidents in light water reactors. RELAP5-3D extended the RELAP5 capabilities to include 3-dimensional analyses. RELAP5-3D models neutronic and fluid flow systems and with greater than 20 years of continuous development, RELAP5-3D has become one of the premier tools for modeling off-normal events in a light water reactor. ATHENA (Advanced Thermal Hydraulic Energy Network Analyzer), complements RELAP5-3D by increasing the fluid option from water to other coolants (e.g., helium, lithium, heavy water, sodium, sodium-potassium, potassium, hydrogen, lead-bismuth, lithium-lead, nitrogen, Flibe, and carbon-dioxide). For the research discussed in this report, ATHENA version 2.24 was used.

3.2.1 Core Analysis Radial Rings

To create the ATHENA model for the MIT design, the core was sectioned into five radial rings. Beginning at the centerline of the core and moving in an outward radial direction, there are the inner, middle, and outer fuel rings. These three fuel rings contain the 127 prismatic blocks of the MIT design and comprise the 11 m^3 volume of the core, while also satisfying the 50/40/10 volume fraction requirement for the fuel, gas, and SiC matrix. In Figure 29, the prismatic blocks have been colored to identify the number of blocks in each ring.

Adjacent to the outer fuel ring is the reflector ring, which is followed by the shield ring. The MIT design does not currently specify physical dimensions or void fractions for the reflector and shield blocks. Furthermore, there is an absence of details regarding the flow rate through these blocks. For this analysis, the reflector and shield blocks have the same physical dimensions as a fuel block, however, the void fraction was reduced 20% in order to provide more material for the block's respective function, i.e., neutron reflection or neutron shielding. While there are coolant channels within the reflector and shield blocks, there is no coolant flow through the reflector and shield rings. This decision was made in order to observe the heat conducted and radiated from the outer fuel ring. Since the design does not specify bypass flow between the core assemblies, this phenomenon was also ignored in the ATHENA model.

3.2.2 Core Unit Cell Representation

Each of the three fuel sections (inner, middle, and outer rings) contains a predetermined number of prismatic type fuel blocks. The fuel blocks are identical in their physical dimension and fuel/coolant/matrix volume fractions. It was thus possible to create a unit cell for the fuel. The unit cell has coolant at its center, a thin layer of SiC matrix material adjacent to the coolant channel, and then a region of fuel material, see Figure 30. The dimensions for the unit cell's coolant channel diameter, matrix thickness, and fuel area are calculated from the prismatic block specifications. The unit cell method greatly simplifies the ATHENA model since the fuel, coolant, and SiC volumes in a fuel ring can be represented by multiplying (1) the unit cell, (2) the number of cells in a prismatic block, and (3) the number of prismatic blocks in a fuel ring.

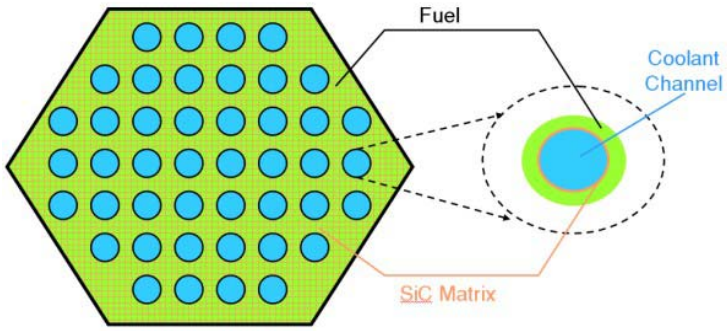

Figure 30: Fuel unit cell for ATHENA analysis.

3.2.3 Core Materials

The design specifies (U, Pu)C as the fuel. However, since fuel fabrication research is ongoing, these initial analyses use uranium-carbide (UC) as the fuel. A literature review revealed several variants of SiC, this research used the properties reported by Nilsson. Pending future material development, it has been proposed that the neutron reflector is composed of titanium-nitride (TiN) and the neutron shield is manufactured from Boron-Carbide (BC). The thermal conductivity of the core materials has a significant impact on the core's thermal performance. The thermal conductivities used in the ATHENA analyses are presented in Figure 31.

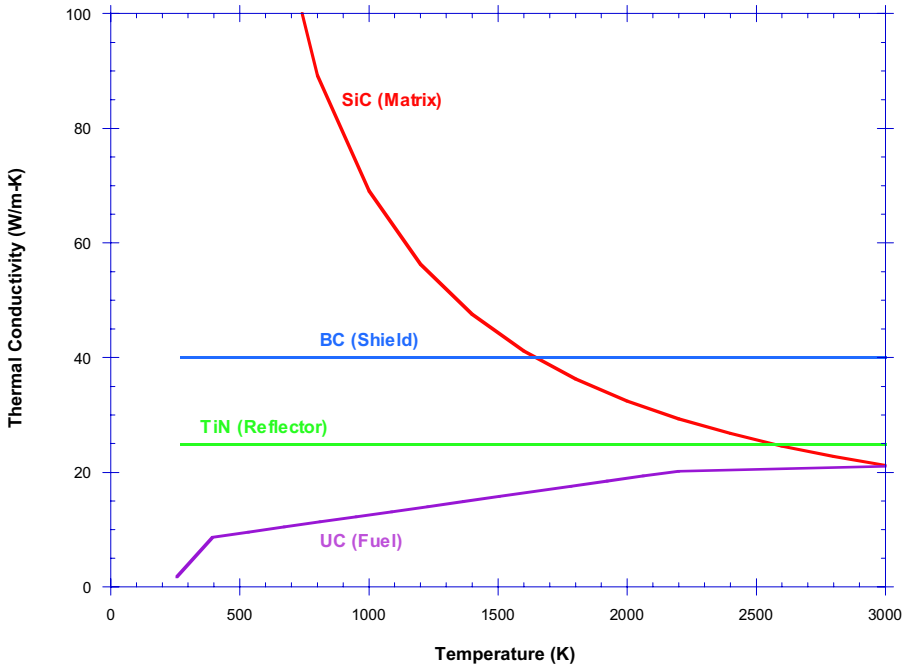

Figure 31: Thermal conductivities for the core components.

3.2.4 Hydraulic Nodalization

The hydrodynamic volumes of the ATHENA model were created using the prototypical reactor vessel configuration shown in Figure 28. As illustrated in Figure 32, coolant enters and exits from the top of the reactor vessel; the inlet and outlet ducts are concentric. The Power Conversion Unit (PCU) was not included in this initial analysis. Instead, inlet and outlet control volumes replace the PCU. Inlet coolant flows down the core barrel and into the inlet plenum where it is directed up through the core fuel rings. The coolant does not flow through the reflector and shield rings, as evidenced by these volumes having only a heat structure in Figure 32. A small component of the inlet flow is directed to a head plenum in order to cool the dome of the outlet plenum. After cooling the dome, the coolant flow is directed towards the inlet downcomer. The outlet plenum in the ATHENA model was scaled to match the size of the outlet plenum in Figure 28. Figure 32 shows that the ATHENA model has reflectors and shields both below and above the core, in agreement with Figure 28. Coolant flow through the core does travel through the axial reflector and shield, however, these components have zero frictional losses so they do not affect the coolant flow rate and thus the pressure drop across the core. The left side of the image in Figure 32 shows that the core assembly sits on a support structure and this structure sits on rail that is attached to the bottom of the reactor vessel. Since the core support structures can conduct heat to the reactor vessel, they are included in the ATHENA model.

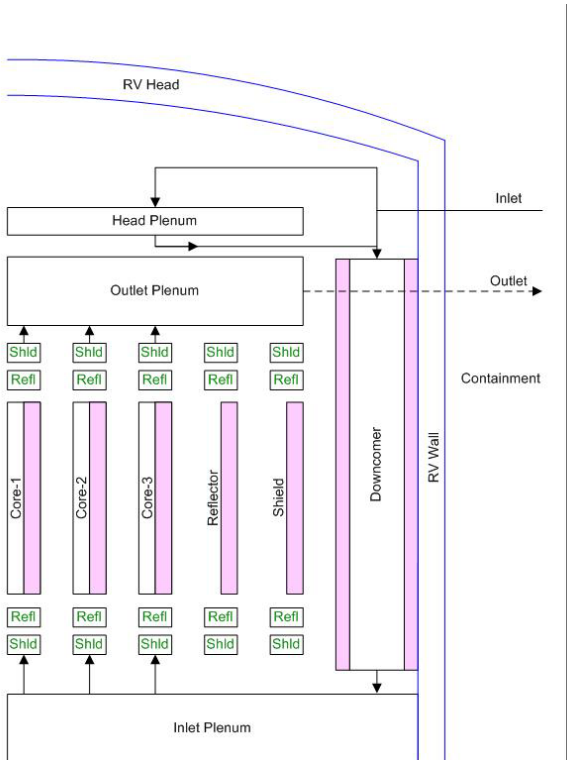

Figure 32: Schematic of the ATHENA hydrodynamic volumes that represent the prototypical in-vessel coolant circuit.

3.2.5 Conduction and Radiation Circuits

In the ATHENA model, heat conduction is allowed within and between the fuel rings. However, it is anticipated that convective heat transfer to the He coolant will dominate heat conduction within the fuel rings. As described earlier, heat is also allowed to conduct from the core to the axial reflector and shield. Heat from the outer fuel ring has a conduction path to the reflector ring, which in turn has a conduction path to the shield ring. The shield ring can conduct heat to the core barrel and to the core support. The selection of gap conductances for the shield ring favors conduction to the core barrel.

The outlet plenum dome is thermally conductive. However, the dome does not have a conduction path to another component. The reactor vessel is comprised of three separate volumes. The head and bottom volumes of the vessel have hemispherical heat structures. These two structures are thermally connected to the cylindrical wall of the vessel. The conduction circuit for the ATHENA model is shown in Figure 33.

The radiation circuit for the ATHENA model includes the reactor vessel wall, bottom, and head. The reactor vessel wall radiates to the cooling panels of the Reactor Cavity Cooling System (RCCS). The RCCS model was taken for an Idaho National Laboratory ATHENA model for the Very High Temperature Reactor. The vessel head and bottom independently radiate to the containment vault ceiling and floor, respectively. Both the ceiling and floor have stainless steel liners in order to prevent thermal decomposition of the containment's concrete wall. Figure 34 presents a schematic of the ATHENA radiation circuit.

3.2.6 Model Specifications

The resulting ATHENA model featured 134 heat structures, 735 mesh points, and 144 hydrodynamic volumes. The primary coolant volume was 6,608 m^3, while the RCCS held 815 m^3 of air. As a result of their differing densities, the He mass was 9,348 kg, while the S-CO_2 mass was 44,402 kg. The air mass of the RCCS was 947 kg.

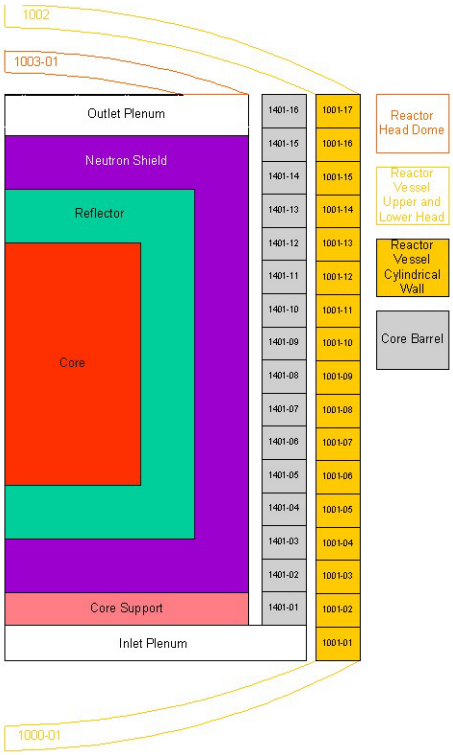

Figure 33: Schematic of ATHENA heat conduction circuit

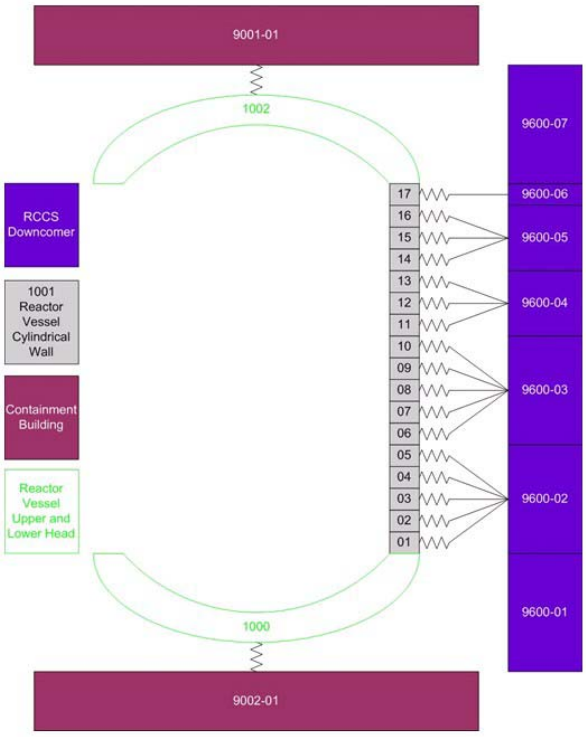

Figure 34: Schematic of radiation circuit for ATHENA model.

3.2.7 Steady State Analysis

The ATHENA analysis with the developed model was performed with He having the variable values provided in Table 5.

Table 5: Steady-State Coolant Parameters

Coolant Parameter	He Option
Inlet Temperature (°C)	490
Outlet Temperature (°C)	842
Mass Flow Rate (kg/s)	330
Outlet Pressure (MPa)	7

The mass flow rate was determined through the use of a control variable. The control variable adjusted the flow into the inlet plenum until the prescribed temperature in the outlet plenum was attained. This procedure was employed in order to verify the pressure drop across the core, as it was reported in the MIT design.

The RCCS is supplied with atmospheric air at 20 °C from the top of the containment vault. Using draft airflow, the RCCS panels absorb the radiated heat from the reactor vessel and direct the heated air upwards, where it is rejected to the atmosphere external to the containment.

As discussed earlier, there was neither gamma nor neutron heating in the reflectors or shields. Any temperature rise in these components was the result of thermal conduction or radiation from the core. Steady-state operation, in terms of constant material temperatures, was determined by observing the air temperature of the containment vault. As a result of the radiation and conduction from the core components and the radiative heat being removed by the RCCS, the reactor vessel wall required an analysis time of 5.3 days in order to achieve steady state heating of the containment vault. The analysis time is the length of the analysis simulation and is different from the computer processing time.

3.3 Simulated LOCA Analysis

The LOCA analysis had the objective of simulating a simultaneous double guillotine break of the inlet and outlet coolant ducts. A control valve was installed in each of the coolant ducts. The valves shared the respective flow areas of the coolant ducts. When the loss of coolant transient is initiated, both control valves instantaneously block flow to the outlet control volume and from the inlet control volume. Flow from the reactor vessel inlet and outlet cooling ducts is allowed to escape into the containment vault.

Simultaneous with the flow control valve operation, the reactor core is SCRAMed. In order to accomplish the SCRAM, a SCRAM reactivity curve from the Seabrook Pressurized Water Reactor (PWR) was input to the ATHENA model. It was recognized that a PWR has a thermal neutron spectrum while the gas fast reactor has a fast neutron spectrum. However, for these initial analyses, the Seabrook PWR SCRAM reactivity curve was considered to be within an acceptable margin of error, given the current design status. The analysis time following the loss of coolant initiation was 50 hrs.

3.3.1 Evolution of the ATHENA Model

With time, the ATHENA model evolved to better represent an actual reactor and to incorporate improvements in the modeling technique. For space consideration, only the major improvements to the model are discussed below. In order to minimize confusion regarding the current state of the model, only the most recent plots of the LOCA response are presented.

3.3.1.1 Heat Transfer Correlations

The initial ATHENA model used the Dittus-Boelter heat transfer coefficient correlation for turbulent flow. However, MIT analyses suggested that the Gnielinski correlation was better for helium forced convection cooling. Thus, one of the goals for this research was to observe the predicted fuel temperatures, when the Dittus-Boelter and Gnielinski correlations were individually selected.

Table 6 presents the steady-state temperatures of the five axial fuel cells for both the Dittus-Boelter and Gnielinski analyses. It is observed in Table 6 that the peak fuel temperature occurs at axial cell 3, which corresponds to the peak power distribution. More importantly, Table 6 illustrates that the Gnielinski correlation is more conservative in its prediction of helium's ability

to transfer heat from the coolant wall. The difference in resulting fuel temperatures for the two correlations is also presented in Table 6.

Table 6: Difference in Dittus-Boelter and Gnielinski-produced Axial Fuel Temperatures

Axial Fuel Cell Number	Dittus-Boelter (C)	Gnielinski (C)	% difference
1	721	748	+ 3.7
2	1116	1223	+ 9.6
3	1330	1462	+ 9.9
4	1300	1388	+ 6.8
5	1029	1051	+ 2.1

The simulated LOCA was performed in order to observe the fuel temperatures resulting from the two heat transfer correlations. Figure 35 presents the LOCA-induced fuel temperatures for using the two heat transfer correlations.

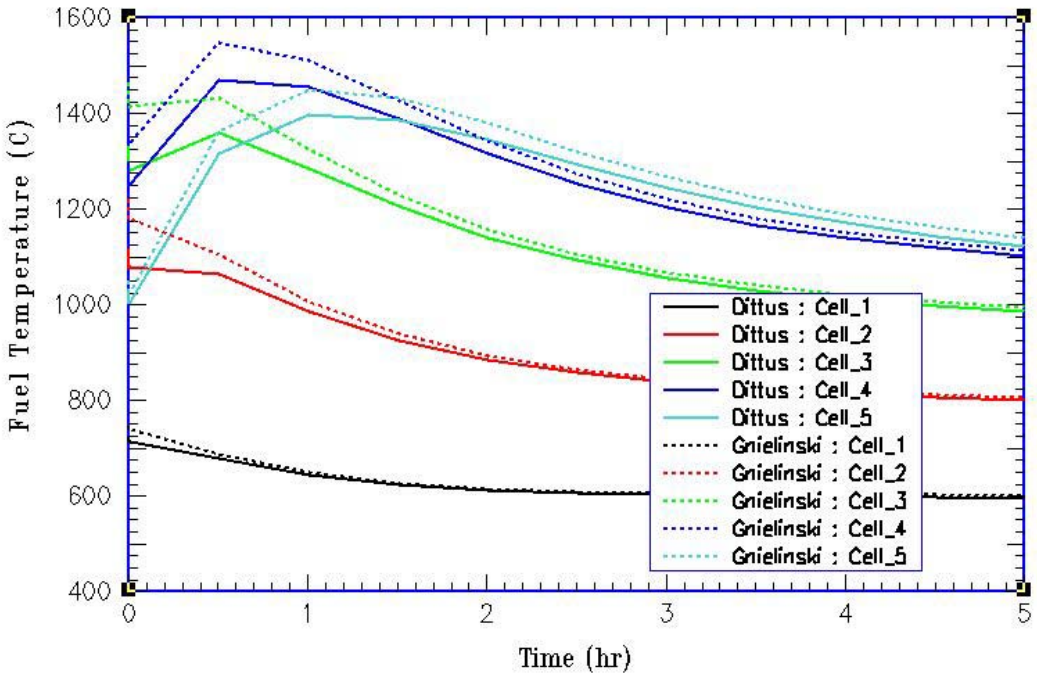

Figure 35: Comparison of LOCA axial fuel temperatures for the Dittus-Boelter and Gnielinski correlations

In Figure 35, the change in slope of the fuel temperature is a result of the guard containment vent valves opening to release guard containment in excess of the pre-determined 1.2 MPa. The valves open when the LOCA is initiated and again when the heat removed from the core increases the cavity's pressure. The guard containment pressure for this analysis is shown in Figure 36. It is this backpressure that gives the helium-air mixture sufficient density to remove

the reactor decay heat without exceeding the fuel design limit of 1650 °C. It is interesting to note in Figure 36 that during the first 1.5 hours of the transient, the guard containment pressure is nearly the same, regardless of the heat transfer coefficient used.

It is observed in Figure 35 that the fuel temperatures resulting from the Gnielinski correlation are considerably different from those resulting from the Dittus-Boelter correlation. Within the first two hours of the transient, the fuel temperature predicted using the Gnielinski correlation does not provide a significant safety margin from the design limit of the fuel. For this reason, the Gnielinski correlation is considered to be more conservative and was thus selected as the default heat transfer correlation for future analyses. That is, a design that provides an acceptable safety margin when the Gnielinski correlation is used will be more conservative than a design that has the same safety margin, but is based on the Dittus-Boelter correlation.

The results presented in Figure 37 were not often discussed in existing LOCA analyses found in the literature. However, Figure 37 is very important because it shows that while natural circulation with a back pressure of 1.2 MPa is sufficient to remove the reactor decay heat, the resulting gas temperature in the guard containment will present severe challenges to the reactor and its supporting materials. Regardless of the heat transfer coefficient used, a guard containment temperature above 500 °C will mostly likely be an obstacle for reactor licensing. The steady-state guard containment temperature is 242 °C.

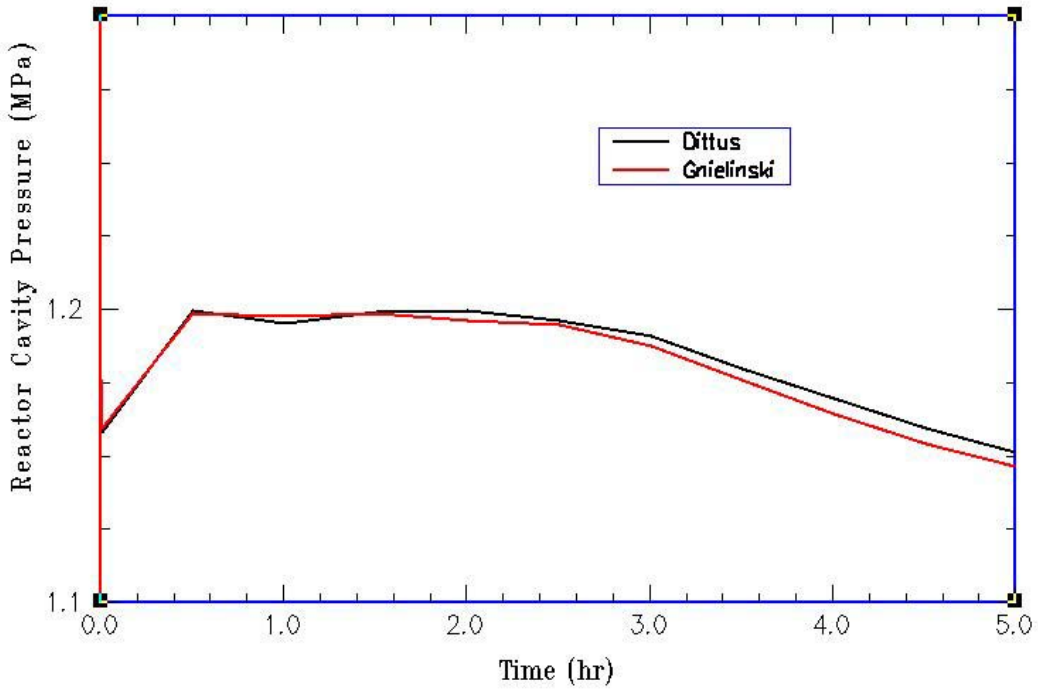

Figure 36: Guard containment pressure during the simulated LOCA with the Dittus-Boelter and Gnielinski correlations

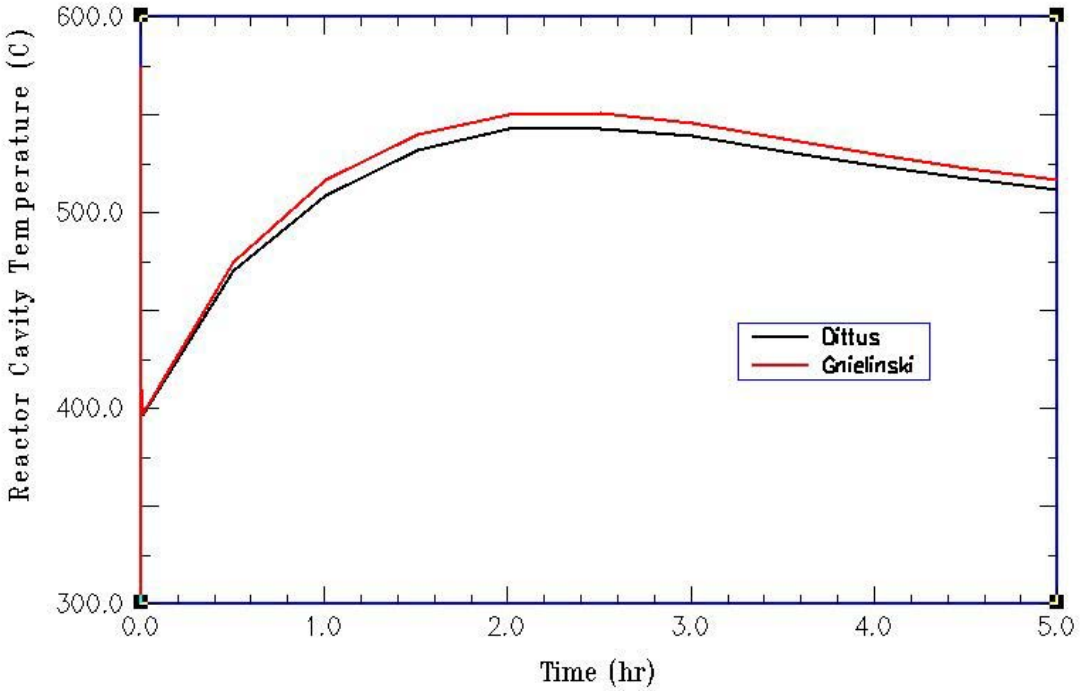

Figure 37: Guard containment temperature during the simulated LOCA with the Dittus-Boelter and Gnielinski correlations

3.3.1.2 Influence of Guard Containment Back Pressure

Given the results in Figure 37, the question arose whether a higher backpressure would decrease the guard containment temperature since it was known that the higher backpressure would reduce fuel temperatures. If the higher backpressure would also reduce the guard containment temperature, then it might offset the additional cost of a higher pressure-qualified guard containment.

Figure 38 presents the resulting fuel temperature for axial fuel cell 4 when the Gnielinski correlation is used and the backpressure is increased to 2 and 3 MPa. It is observed in Figure 38 that the fuel temperature is no longer a concern at the higher guard containment backpressures. Unfortunately, the higher guard containment back pressure is more efficient at removing decay heat from the reactor core, but it simply moves this heat from the core and into the guard containment, as shown in Figure 39. That is, the heating rate and level of the guard containment increase with increasing back backpressure.

3.3.1.3 Water Decay Heat Removal Loop

It was hypothesized that the addition of a natural circulation water-cooled Decay Heat Removal Loop (DHRL) would provide an advantage of a lower guard containment temperature while maintaining the 1.2 MPa backpressure of the base case.

A generic DHRL was created using a piping loop, pressurizer for the loop, pool of water mounted on top of the containment building, and two heat exchangers (refer to Figure 40). A 6

m length finned heat exchanger was attached to the lower loop section that resided within the guard containment. The upper loop section had two 4 m length vertical finned heat exchangers that were submerged in the containment top-mounted water pool. The difference in height between the upper and lower heat exchangers, in addition to one side of the loop having a longer length, resulted in the establishment of natural circulation within the DHRL loop.

The water pool atop the containment building served as a heat sink and this pool was allowed to evaporate water to the air atmosphere external to the containment building. The initial temperature and pressure of the pool were 20 °C and 0.1 MPa, respectively. The DHRL pressurizer maintained a pressure of 4 MPa in the piping loop. The initial temperature of the water in the loop was 20 °C. During the LOCA transient, natural circulation in the DHRL established an average flow rate of 10 kg/s or 0.2 m/s.

Figure 41 presents the resulting fuel temperatures for the DHRL analysis. The figure includes temperatures for the base Gnielinski case and the Ginielinski model with the DHRL. It is observed in Figure 41 that the fuel temperature for the DHRL case exceeds the design temperature limit of 1650 °C. The higher fuel temperatures for the DHRL case suggest that the guard containment temperatures and pressures are less than the values for the base Gnielinski case. Figure 42 indeed reveals that the DHRL case has a considerably lower guard containment temperature.

The prospect of using a high backpressure in the reactor cavity to maintain heat transfer efficiency during a LOCA seems very promising. The simple physics is that by maintaining a high density of the air-helium mixture, one can adequately remove the decay heat from the reactor without any active systems. However, the Ideal Gas Law intervenes and when the backpressure of the guard containment increases while maintaining the same volume, the temperature of the guard containment likewise increases.

It was imagined that a simple solution would be to add cooling to the guard containment so that the material within the guard containment did not suffer integrity losses due to the high thermal loading. It was simple to add a passive water loop that used natural circulation to remove a considerable amount of heat from the guard containment during the LOCA transient. However, the fundamental law was still in place: if you decrease the guard containment temperature, you consequently decrease the pressure, which lowers your gas density and negatively impacts its capacity to remove heat from the reactor.

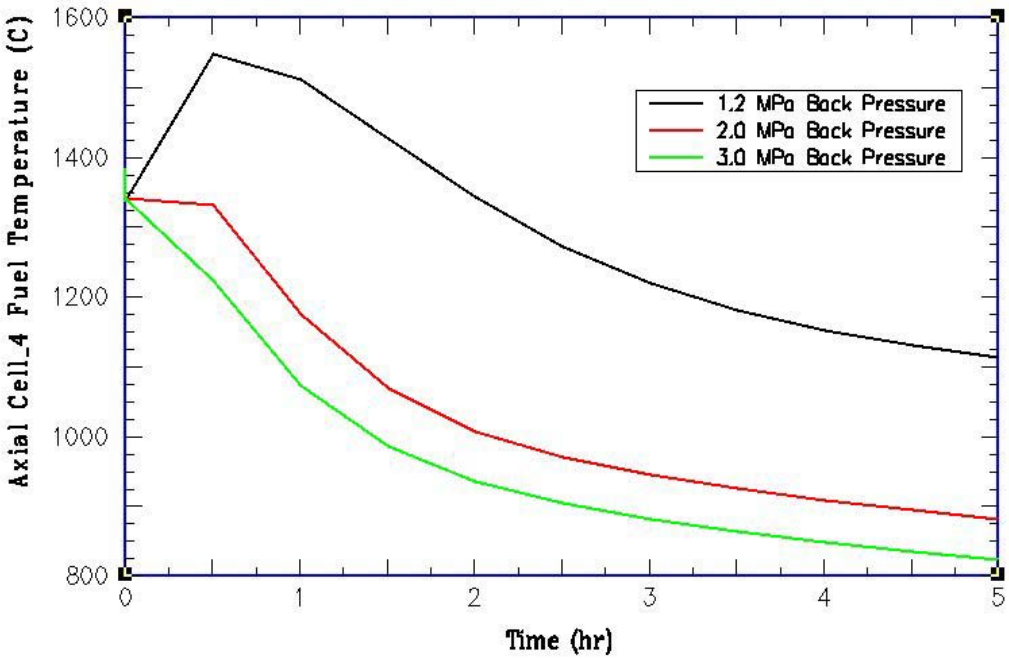

Figure 38: Fuel temperature as a function of increased guard containment backpressure.

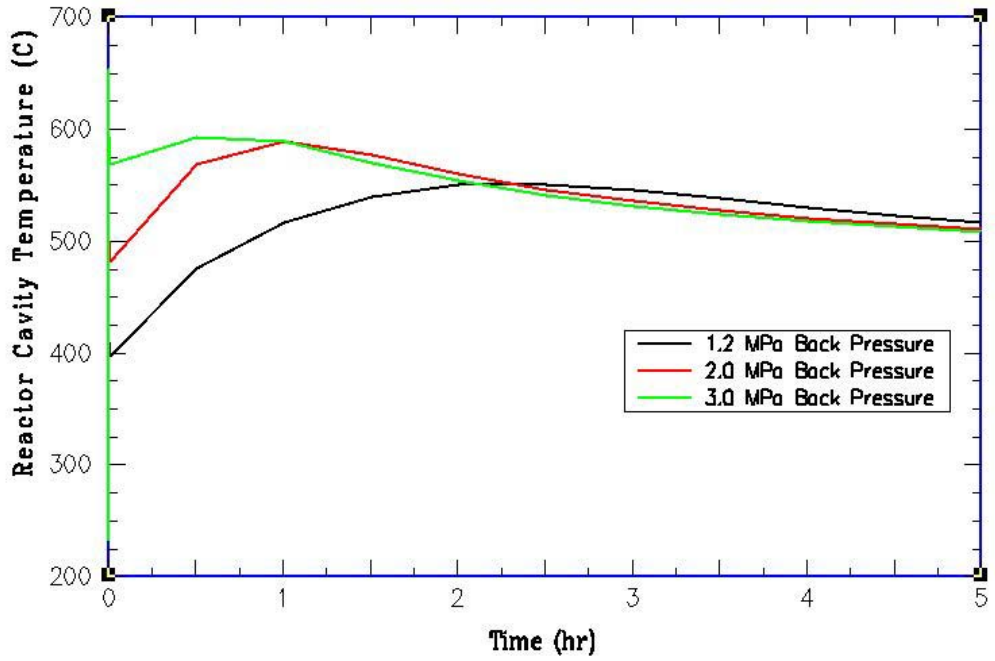

Figure 39: Guard containment temperature as a function of increasing backpressure.

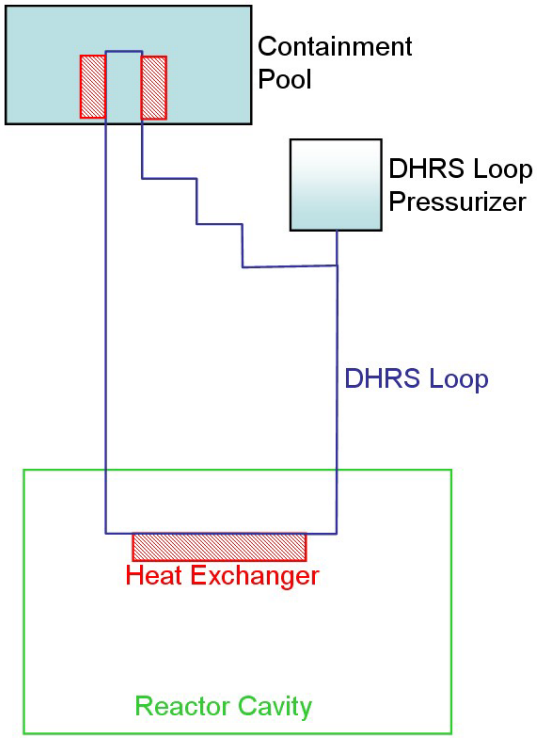

Figure 40: Schematic of natural convection water-filled decay heat removal loop

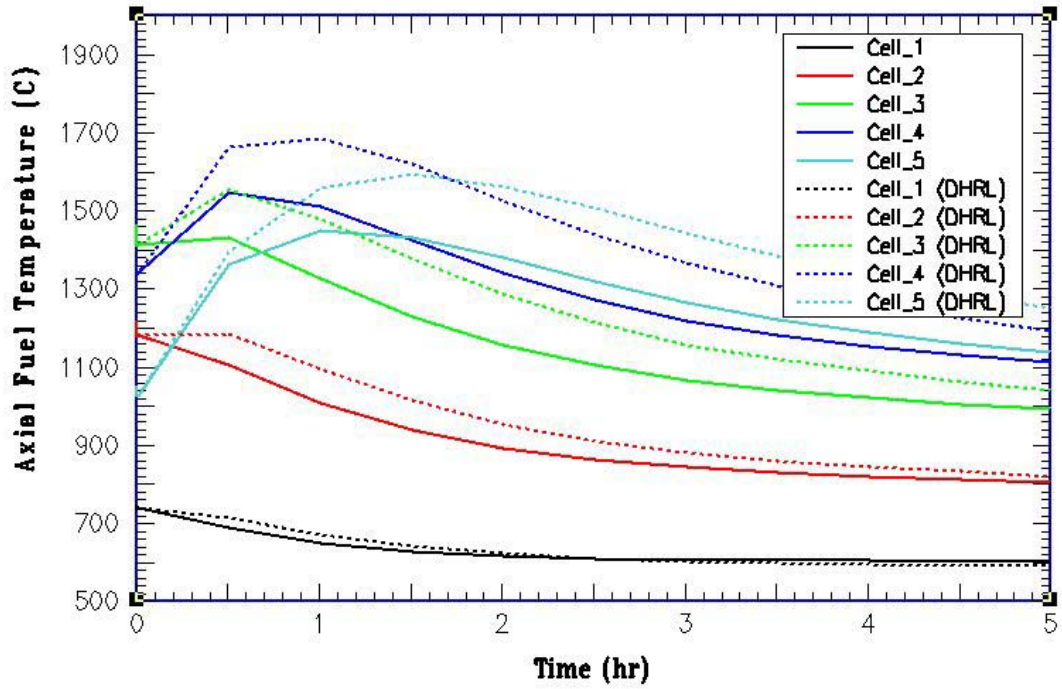

Figure 41: Fuel temperature with and without natural circulation water-filled decay heat removal loop

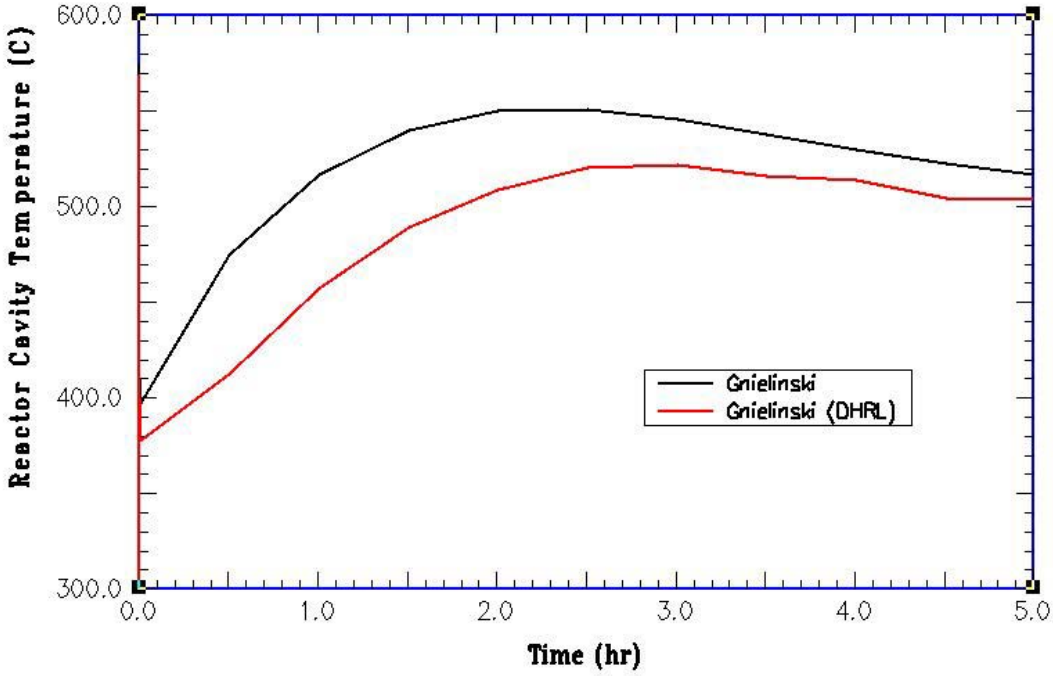

Figure 42: Guard containment pressure with and without natural circulation water-filled decay heat removal loop

3.3.1.4 Radial Peaking Factor

The initial ATHENA model included a core axial height of 1.7 m. The model divides this height into five axial cells and an axial power profile that has a cosine distribution with a peaking factor of 1.25. A schematic of the axial fuel cells and the axial power distribution is shown in Figure 43. It was understood that the assumption of a flat radial profile and the omission of hot channels within the core would yield optimistic results. Thus, a peaked radial profile of 1.3 was added to the model. The addition of this radial profile caused the steady-state analysis to produce fuel temperatures that exceeded the design basis. To compensate for this effect, flow orificing was added to the inlet plenum. Figure 44 shows the fuel temperatures before and after the flow orificing. The use of flow orificing increases the pressure drop across the core from 14 kPa to 73 kPa, with a corresponding increase in the pumping power from 1 to 5.5 MW; approximately 0.9% of the thermal power.

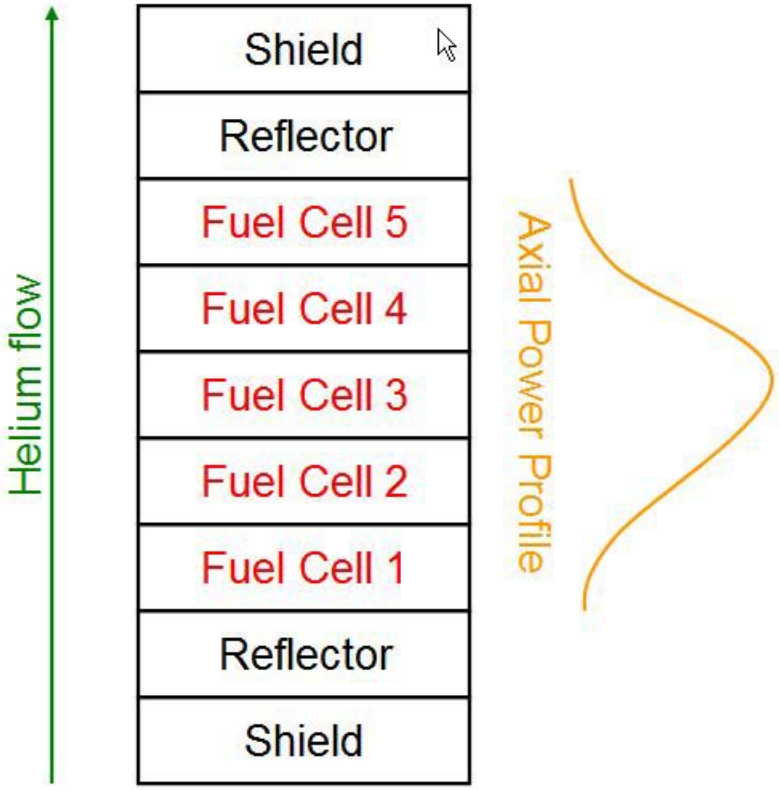

Figure 43: Axial cells of the fuel ring heat structure.

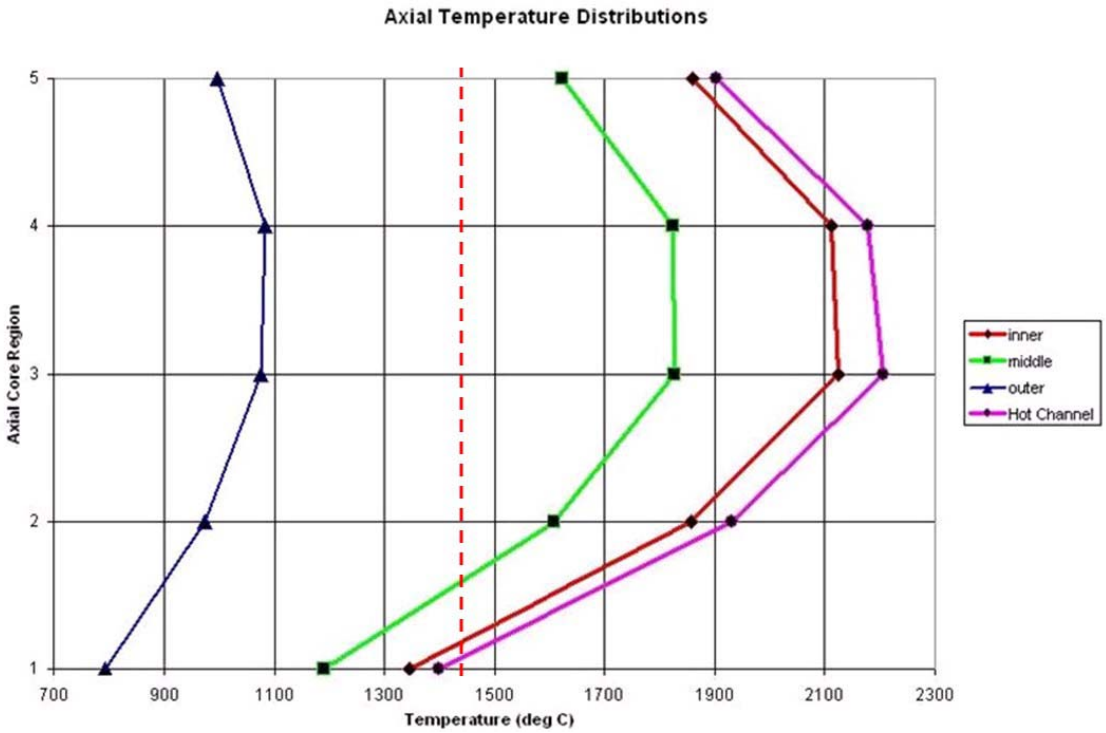

Figure 44: Fuel temperature with radial peaking - prior to inlet plenum orificing

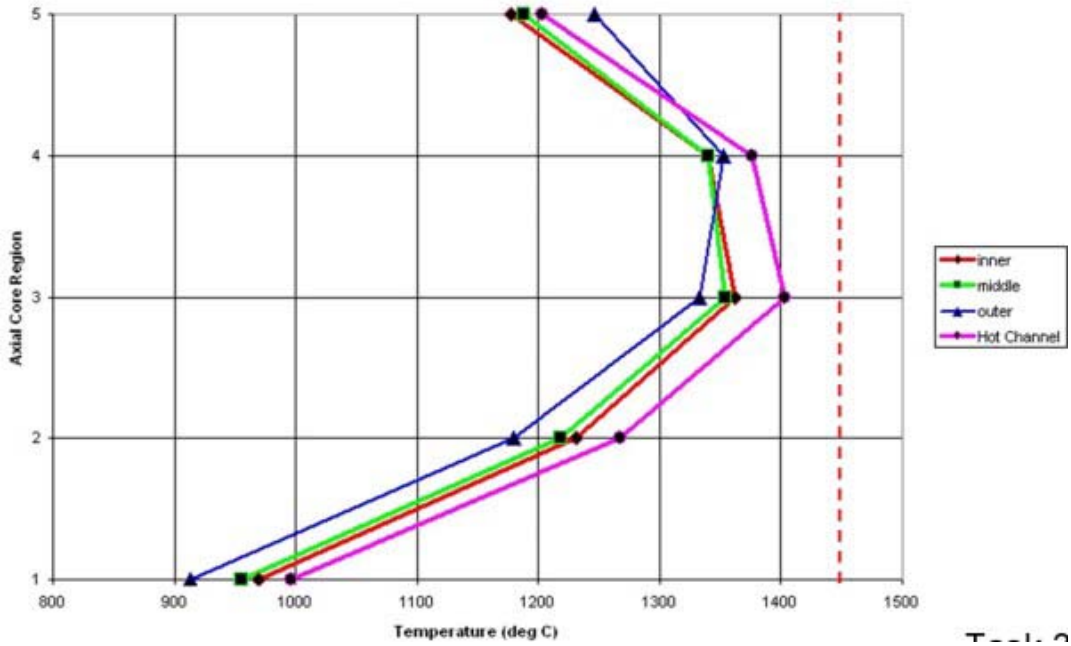

Figure 45: Fuel temperature with radial peaking - after performing inlet plenum orificing

3.3.1.5 SiC Thermal Conductivity Investigation

A literature review suggested that SiC thermal conductivity decreases between one-third and one-half when the material is irradiated. Available data (Figure 46) imply that the change in thermal conductivity can increase the fuel temperature by as much as 150 °C, when the thermal conductivity is decreased by one-third. With the fast flux of approximately 10^{15} n/cm^2-s, the loss of SiC thermal conductivity would occur within weeks of the reactor's operation. Analyses were initiated to examine the effects of SiC thermal conductivity on LOCA-induced fuel temperature and guard containment backpressure. However, these analyses were not completed prior to the NERI project's conclusion.

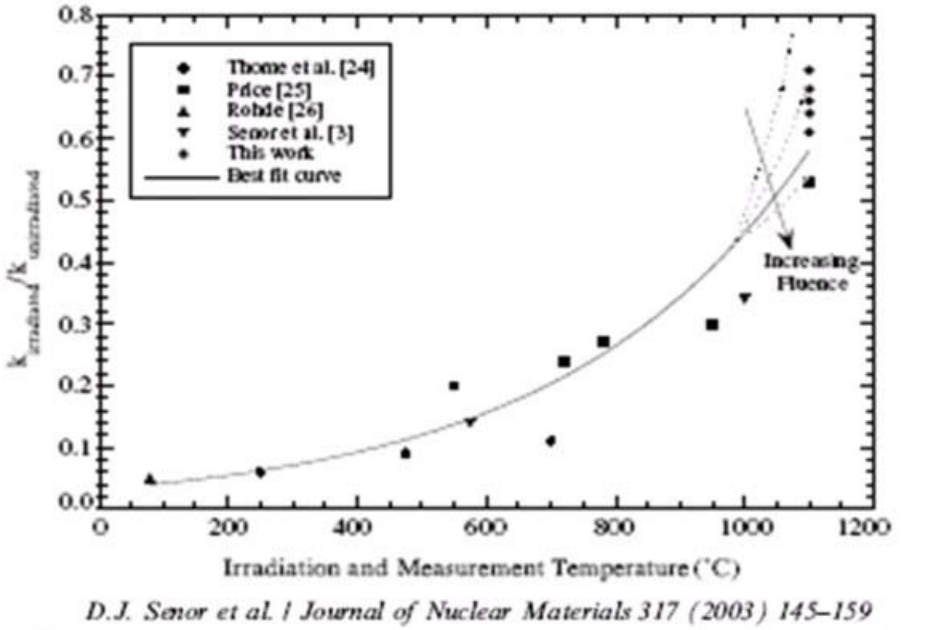

Figure 46: SiC loss of thermal conductivity as a function of irradiation

3.3.1.6 Containment – RCCS Interface Modeling

A noticeable deficiency in the ATHENA LOCA analysis is the fact that ATHENA homogenizes the state values in a hydrodynamic volume. The consequence of this homogenization is that the convective heat transfer from the guard containment to the RCCS and the mixing of the reactor helium and the guard containment air are expected to be considerably underpredicted. An effort was initiated to create a Computational Fluid Dynamics (CFD) model of the reactor vessel, guard containment, and RCCS. The objective was that the CFD model would provide velocity profiles that could be input into ATHENA for the temperature calculations. This effort was approximately 20% complete with the NERI project concluded.

3.4 Conclusions

The principle objective of this research was to develop a realistic model of a prototypical gas fast reactor design and to use that model to examine the reactor's response during a simulated design basis accident. From the discussions presented, it is concluded that the current ATHENA model has considerably evolved beyond the simple hydrodynamic volumes and heat structure

assemblies that are typical of initial design studies. Efforts were underway to increase the model's accuracy and correlation to reality.

The study of the LOCA scenario produced mixed results. It was observed that the design could survive the LOCA if there were sufficient backpressure in the guard containment. However, this survival is questioned when real world effects of irradiation, radial power profiling, and material thermal load limits are taken into consideration. On the other hand, it is realized that the current model underpredicts the convective heat transfer within the guard containment.

The general conclusion is that the current model provides a first order examination of the LOCA scenario. Improvements to the model in order to yield higher accuracy predictions were underway and need to be continued before it can conclusively be stated that the gas fast reactor design can completely survive a LOCA.

References

1 J. F. Briesmeister, .MCNPTM.A General Monte Carlo N-Particle Transport Code,. Los Alamos National Laboratory report LA-12625-M, Version 4B (March 1997).

2 R. L. Moore, B. G. Schnitzler, C. A. Wemple, R.S. Babcock, and D. E. Wessol, "MOCUP: MCNP-ORIGEN2 Coupled Utility Program," INEL-95/0523(September 1995).

3 A. G. Croff, .A User's Manual for ORIGEN2 Computer Code,. Oak Ridge National Laboratory report ORNL/TM-7175 (July 1980).

4 D. B. Pelowitz, ed., "**MCNPX** User's Manual Version **2.5**.0," Los Alamos National Laboratory report, in press (February 2005).